

Conformal Vacuum of $dS_4 \times \mathbb{R}$ with Oppositely Oriented Boundaries

Lucas K. Kovalsky and Shivesh Pathak

*Quantum Algorithms and Applications Collaboratory,
Sandia National Laboratories, Livermore, CA, USA*

Kyle Ritchie

*Leinweber Institute for Theoretical Physics and Department of Physics,
University of California, Berkeley, California 94720, USA and
Quantum Algorithms and Applications Collaboratory,
Sandia National Laboratories, Livermore, CA, USA*

Abstract

We derive a $dS_4 \times \mathbb{R}$ quotient spacetime that is asymptotically dS_4 , where the quotient makes its past boundary oppositely oriented relative to its future boundary. This introduces a lightlike singularity that severs the antipodes of the spacetime and simplifies its global vacuum to a trivial product on antipodal static patches. We show that this state is conformal to the vacuum of an infinite orientable cover of a non-orientable AdS_3 spacetime with an S^2 bundle. The vacuum's separability extends to its holographic dual, which is a product of Cardy states. We find that this candidate dS_4 vacuum state is perturbatively unstable within quantum gravity due to a vanishing Hagedorn temperature.

CONTENTS

I. Introduction	3
II. NO-AdS ₃	5
A. Construction	5
B. The Boundary of NO-AdS ₃	10
C. Holography of NO-AdS ₃	12
D. Instability of NO-AdS ₃ to Quantum Gravity Dynamics	19
E. NO-(AdS ₃ × S ²) Construction	19
III. OB-dS ₄ × ℝ	22
A. OB-dS ₄ × ℝ Construction	23
B. The Bulk/Boundary Correspondence	27
IV. Discussion	29
A. NO-AdS ₃	30
1. Iwasawa and Cartan coordinates	30
2. Mobius construction	32
3. Torus boundary	33
B. NO-(AdS ₃ × S ²) as two glued patches	34
C. dS ₄ × ℝ Bulk Isometry Group and σ	35
D. OB-dS ₄ × ℝ Poincaré Patch Derivation	36
E. Rindler-AdS ₃ × S ² ≅ Static-dS ₄ × ℍ ¹	37
References	39

I. INTRODUCTION

De Sitter spacetime with d -dimensions (dS_d) is a maximally symmetric, time-dependent vacuum spacetime with a constant radius of curvature, ℓ , specified by its positive cosmological constant, $\Lambda \propto \ell^{-2}$. The positive cosmological constant produces an accelerating universe that limits timelike observers in dS_d to only have access to part of the spacetime. Antipodal observers inhabit causally independent static patches, and their future and past lightcones intersect behind cosmological horizons of area $\propto \ell$. This causal structure produces a Euclidean vacuum that is entangled across the bifurcated horizon in a thermofield double state with temperature $\propto \ell^{-1}$ [1–6].

This entanglement structure is difficult to describe within quantum gravity because accessing observables supported beyond cosmological horizons generally requires access to the global isometries of a spacetime [7–9]. By contrast, a string theory is more naturally restricted to the local isometries of a static patch. The holographic perspective is similarly difficult. The fact that timelike observers do not have causal influence over all of the spacetime means that de Sitter possesses spacelike boundaries, which prevent the more straightforward unitary holographic duality that timelike boundaries can offer. This means that few lessons can be applied from the AdS/CFT correspondence without significant modification [10, 11].

Compounding matters further, de Sitter spacetime exhibits exotic properties seemingly at odds with quantum gravity, including that it may support only a finite Hilbert space [12–19] and its graviton propagator diverges [20–24]. As a result, vacuum states in de Sitter are notoriously difficult to define within quantum gravity and are frequently found to be tachyonic and unstable [25–29].

The more natural candidates for holographic boundaries in de Sitter are the null cosmological horizons of its static patches [4]. Exploring these has led to the so-called “monolayer” and “bilayer” proposals. [30–38]. Here we will instead flip the orientation of the past and future boundaries to disentangle antipodal static patches. This will allow restricting access of timelike observers to the local isometries of their past and future Poincaré patches. Importantly, since the boundaries of this spacetime individually remain the same as dS_4 , the resultant bulk geometry will be a candidate vacuum state geometry within quantum gravity.

To construct the new $dS_4 \times \mathbb{R}$ spacetime (which we refer to as OB- $dS_4 \times \mathbb{R}$ with the ‘OB’ indicating “oppositely oriented boundaries”), we will use a foliation of a non-orientable $\mathbb{R}^{2,5}$

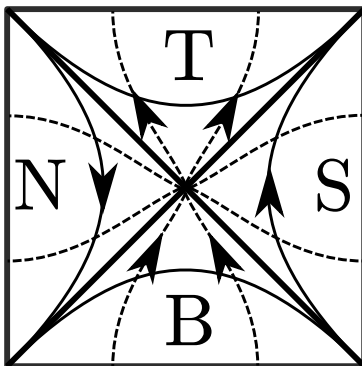


FIG. 1. The Penrose diagram of dS_d with static patches ('N' and 'S') at its antipodal worldsheets and top and bottom ('T' and 'B') time-dependent patches. While the north (N) and south (S) static patches are disjoint, they share their future and past cones behind a cosmological horizon indicated by the thick diagonal crossing lines. The thin filled (dashed) lines correspond to timelike (spacelike) geodesics in the static patches.

lightcone. This lightcone is useful because it can also be foliated by a non-orientable AdS_3 bundle fibered by S^2 in the same manner as a better-known construction for (orientable) $AdS_3 \times S^2$ and $dS_4 \times \mathbb{R}$ (with similarly oriented boundaries). Their common foliation of $\mathbb{R}^{2,5}$ establishes a conformal relationship between Rindler wedges of $AdS_3 \times S^2$ and static patches of $dS_4 \times \mathbb{R}$. In its standard form, the conformal map takes the asymptotic boundary of AdS_3 to the static patch worldsheet of $dS_4 \times \mathbb{R}$ and is not extendable to both antipodal static patches. The holographic implications, if any, are difficult to determine [39, 40]. By instead considering the conformal map from an infinite orientable cover of non-orientable AdS_3 fibered by S^2 , we will find that we are able to leverage the new global topology to effectively extend this conformal map to both antipodal static patches of $OB-dS_4 \times \mathbb{R}$ with a well-defined holographic boundary.

The non-orientable AdS_3 spacetime is a recently discovered orientifold of one of its asymmetric double covers [41]. Its bulk is locally indistinguishable from AdS_3 . Much like BTZ, it is only possible to derive it in three dimensions and is an exact solution of Einstein's equations (i.e. it does not have singularities). Upon non-trivially fibering with S^2 , we will find that this space is key to determining the properties of $OB-dS_4 \times \mathbb{R}$.

Finally, we will find that the separable vacuum of $OB-dS_4 \times \mathbb{R}$ is perturbatively unstable to

excitation due to a vanishing Hagedorn temperature. It may decay to one of two degenerate $dS_4 \times \mathbb{R}$ spacetime with similarly oriented boundaries. The latter spacetimes share the same asymptotic boundary as dS_4 , but with static patches that are independently conformal to Rindler wedges of orientable $AdS_3 \times S^2$.

This paper is organized as follows: in Section II we review the properties of non-orientable AdS_3 and its separable Euclidean vacuum on antipodal Rindler wedges. In Section III we derive OB- $dS_4 \times \mathbb{R}$ and show that its Euclidean vacuum must similarly be separable on antipodal static patches. We then introduce the conformal map between one of its static patches and a Rindler wedge of non-orientable AdS_3 fibered by S^2 . The separability extends this conformal map piece-wise to both antipodal static patches. This allows us to develop a global holographic correspondence between bulk dS_4 and a conformal field theory, utilizing the AdS_3/CFT_2 correspondence. Finally, we discuss the implications of our derivation in Section IV.

II. NO- AdS_3

In this section we review the construction of non-orientable AdS_3 (NO- AdS_3) from a quotient of a double cover of AdS_3 . We discuss its isometry group and the structure of its asymptotic boundary. We emphasize that, when the bulk is restricted to a Rindler patch, states in the dual theory can be characterized by Cardy states associated with the two fixed-point lines on the boundary of the Rindler wedge.

A. Construction

The metric for AdS_3 in global coordinates is commonly written as

$$ds^2 = \ell^2(-\cosh^2(\rho)dt^2 + d\rho^2 + \sinh^2(\rho)d\phi^2), \quad (1)$$

where $\rho > 0$, $\phi \in [0, 2\pi)$, and $t \in \mathbb{R}$ (for its universal cover) with ℓ equal to AdS_3 's radius of curvature.

It turns out that AdS_3 can be rewritten in terms of global coordinates that align with the Iwasawa decomposition of $SL(2, \mathbb{R})$ instead, which corresponds to the group manifold of

AdS₃:

$$ds^2 = \ell^2 \left(-d\theta^2 + dx d\theta - \frac{2x}{r} d\theta dr + \frac{dr^2}{r^2} \right), \quad (2)$$

where $r > 0$, $\theta \in [0, 2\pi)$, and $x \in \mathbb{R}$ (see Appendix A for more details). r is spacelike, θ is timelike, and x is lightlike. Note that the (simply connected) boundary is located both at $r = 0$ and $r = \infty$, where $r = 0$ is a one-dimensional patch and $r = \infty$ is a two-dimensional patch.

In this coordinate system a cylinder can be explicitly seen to be defined in θ and x coordinates and it is thus straightforward to change the topology of that submanifold to a Mobius strip: $\sigma(x, \theta) = (-x, \theta + 2\pi)$. It is not possible to find such a cylinder in the usual (ρ, r, θ) coordinates because any angular coordinate will invariably be conical and introduce a conical defect after a twist. The value of the Iwasawa decomposition metric is that this twist can be performed without introducing a singularity in the bulk, since $r = 0$ is also at the boundary. The lack of singularity can also be explained by the fact that there exists a (branched) double cover of AdS₃ containing this twist in the form of a $\sigma \equiv \mathbb{Z}_2$ subgroup [41], and NO-AdS₃ can also be derived by quotienting this double cover by the \mathbb{Z}_2 .

Yet another way to derive NO-AdS₃ is by using its embedding in $\mathbb{R}^{2,2}$. We review this procedure as it is similar to the one we use to derive the OB-dS₄ \times \mathbb{R} spacetime. Consider the embedding space $\mathbb{R}^{2,2}$ with metric $-du^2 - dv^2 + dx^2 + dy^2$. In null coordinates $(u + x, v + y, v - y, x - u) \equiv (A, B, C, D)$ the metric is

$$ds^2 = dAdD - dBdC. \quad (3)$$

Since the two sides of the lightcone in $\mathbb{R}^{2,2}$ are identical, the hyperboloid $AD - BC = \mp\epsilon$ corresponds to an AdS₃ on either side of the $\mathbb{R}^{2,2}$ lightcone.

This allows for a double cover of the spacetime to be defined, whose quotient will turn out to be equivalent to a single non-orientable cover [41]. Note that the equivalence of the two sides means that Poincaré patches on one side of the lightcone can be brought to the other side isometrically (i.e. rigidly so that $(A, B, \epsilon) \rightarrow -(A, B, \epsilon)$). For $d \neq 2$, this is not possible for AdS _{$d+1$} embedded within $\mathbb{R}^{2,d}$, since the embeddings on opposite sides of the $\mathbb{R}^{2,d}$ lightcone are not isometrically related. Moreover, it is only for $d = 2$ that the isometry group factorizes into a product of two SL(2, \mathbb{R})s. Relatedly, working in AdS₃ Poincaré coordinates (τ, x, y) , there are two ways of isometrically transforming Poincaré patches from one side of the lightcone to the other: 1. a simple reflection which takes $ds^2(\tau, x, y) \rightarrow -ds^2(\tau, x, y)$, or

2. a reflection with an exchange which takes $ds^2(\tau, x, y) \rightarrow -ds^2(x, \tau, y)$. By performing 1 and then 2, we can define a disjoint Poincaré patch on the *same side* of the $\mathbb{R}^{2,2}$ lightcone, and thereby define a new AdS_3 , as two glued Poincaré patches related by $\tau \leftrightarrow x$ exchange. This AdS_3 will be geometrically indistinguishable from regular AdS_3 but will inherit a non-trivial topology.

While this looks simple enough in Poincaré coordinates, it requires a bit of extra work to relate the two Poincaré patch domains consistently to the embedding coordinates under these isometries, which is necessary to obtain the correct gluing between them.

The usual Poincaré coordinates (τ, x, y) are defined in the flat embedding coordinates (A, B, C, D) as $A = 1/y$, $B = (\tau - x)/y$, $C = (\tau + x)/y$ and $D = (-\epsilon + BC)/A = (\tau^2 - x^2)/y - \epsilon y$, where $\epsilon > 0$. We begin by considering two copies of a Poincaré patch, where one is taken to the AdS_3 hyperboloid on the other side of $\mathbb{R}^{2,2}$'s lightcone by the map $\sigma(A, B, C, D) \rightarrow (-A, -B, C, D)$. To do this we define \pm branches so that they correspond to Poincaré patches under the pre-image and image of σ , respectively, in $\mathbb{R}^{2,2}$:

$$A = \pm 1/y, \quad B = \pm(\tau - x)/y, \quad (4)$$

$$C = (\tau + x)/y, \quad D = (\tau^2 - x^2)/y - \epsilon y. \quad (5)$$

Note that this makes $(AD - BC) = \mp\epsilon$, as expected from the pre-image and image of σ , which exchanges the two sides of the $\mathbb{R}^{2,2}$ lightcone. Also note that $y > 0$ on both branches.

As a result, the metric of the two Poincaré patches looks different compared to a pair of Poincaré patches of regular AdS_3 :

$$ds^2 = \begin{cases} y^{-2}(-d\tau^2 + dx^2 + \epsilon dy^2) & \text{for } y > 0, \\ y^{-2}(d\tau^2 - dx^2 - \epsilon dy^2) & \text{for } y > 0. \end{cases} \quad (6)$$

Specifically, these two metrics have opposite signature, which is expected, because of our earlier setup associating the two branches with opposite sides of the $\mathbb{R}^{2,2}$ lightcone. This also means that the domains of these two Poincaré patches do not overlap in the embedding space, despite their domains being equal in the embedded Poincaré coordinates, since each of the \pm hyperboloids contain $A > 0$ and $A < 0$ regions.

We proceed to isometrically transform the second (“−” branch) Poincaré patch again so that it moves to the same side of the lightcone as the other Poincaré patch. We use the embedded coordinates to accomplish this by setting $y \rightarrow \pm y$ and $(\tau + x) \rightarrow \pm(\tau + x)$. This

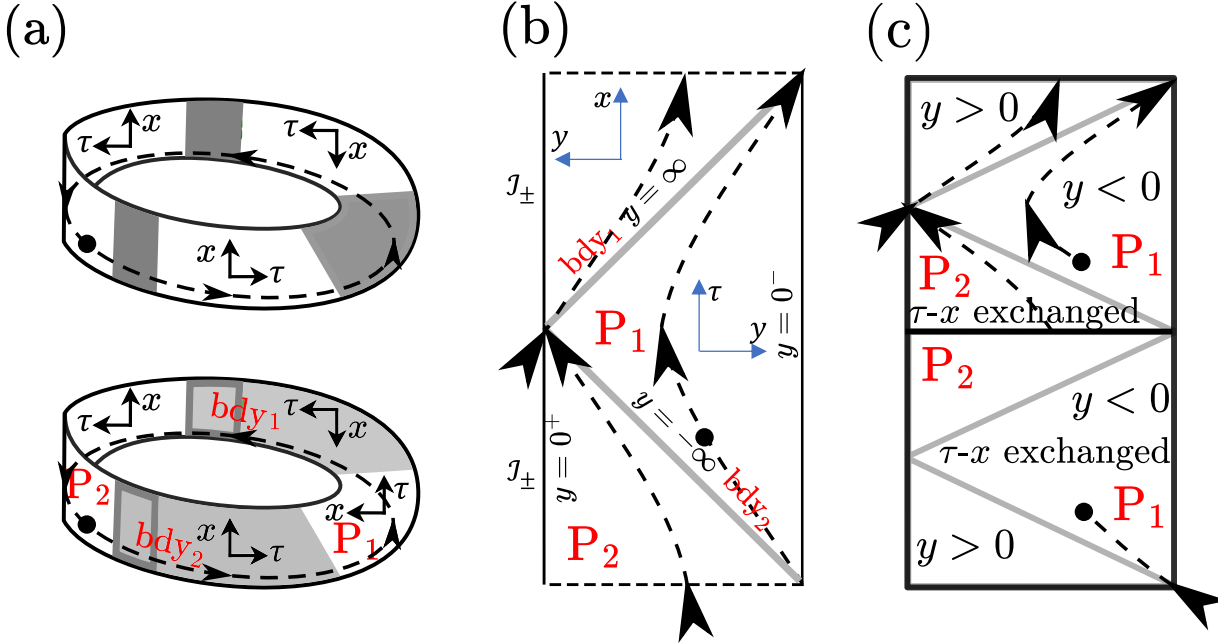


FIG. 2. NO-AdS₃ contains (a) a Möbius strip topology that can be seen in the two Poincaré patches. A timelike loop in its two (b) Poincaré patches returns to itself but with opposite orientation. This can be seen more clearly through its (c) orientable double cover since $\tau - x$ are exchanged after the equivalent loop.

sets $A = 1/y$, $B = (\tau - x)/y$, $C = (\tau + x)/y$ and $D = (\tau^2 - x^2)/y \mp \epsilon y$, where $y \geq 0$. Notice that these are the same as the usual Poincaré coordinates except for the factor of $\mp \epsilon y$ in D and the additional specification that $y \geq 0$. Therefore, from the perspective of the embedding (A, B, C, D) coordinates, this involves both a simple $(A, B, C, D) \rightarrow (-A, -B, C, D)$ reflection across its lightcone and an $\epsilon \rightarrow -\epsilon$ reflection along with $y \geq 0$.

The effect of the ϵ changing sign on the Poincaré metric turns out to be an exchange between τ and x alongside the signature flip:

$$ds^2 = \begin{cases} y^{-2}(-d\tau^2 + dx^2 + \epsilon dy^2) & \text{for } y > 0, \\ y^{-2}(d\tau^2 - dx^2 + \epsilon dy^2) & \text{for } y < 0. \end{cases} \quad (7)$$

This corresponds to two Poincaré patches on the same side of $\mathbb{R}^{2,2}$, which have τ and x exchanged, which are now qualified to be two patches of a single AdS₃.

These two patches define a non-orientable AdS₃ which we refer to as NO-AdS₃. Since these two patches have exchanged τ and x , it can be found that a timelike observer which

makes a single loop returns to themselves with opposite orientation in its tangent space; a consequence of the Möbius topology [41] (see Fig. 2a). Explicitly, for a closed cycle in the (A, B) plane, e.g. $(A, B) = (R \cos \Theta, R \sin \Theta)$, one finds that $(\partial_A, \partial_B) \rightarrow (-\partial_A, -\partial_B) \rightarrow (\partial_A, \partial_B)$ as $\Theta \rightarrow \Theta + 2\pi \rightarrow \Theta + 4\pi$. A Penrose diagram of this spacetime with the two Poincaré patches is shown in Fig. 2b, though this is not strictly a compactification to the Einstein static universe due to the boundary topology, as we explain in the next section. Its orientable double cover can also be shown as in Fig. 2c.

In global coordinates (ρ, t, ϕ) , we have constructed an identification between two AdS_3 spacetimes under $\sigma(\ell, \rho, t, \phi) = (i\ell, \rho + i\pi/2, \phi + \pi, t + \pi)$ [41]. The Wick rotation of the ρ and the ℓ follow each other resulting in an overall minus sign, in much the same way that the opposite signature second branch Poincaré patch above was brought back to a consistent signature with the first Poincaré patch, though now oppositely oriented.

Note that it is not possible to write a global metric of a non-orientable manifold. This is because such a manifold always contains a Möbius strip topology, which requires three overlapping patches with transition functions (see the top of Fig. 2a) or two non-overlapping patches with gluing rules (see the bottom of Fig. 2a). The Poincaré patches correspond to the latter (Fig. 2b).

However, it is possible to write a global metric for the orientable double or universal cover of a non-orientable manifold. For NO- AdS_3 , its universal cover can be written by unrolling the θ in the compactification of the Iwasawa metric (Eq. A21):

$$ds^2 = \frac{dr^2}{r^2} - d\theta^2 - \chi d\theta dr + rd\chi d\theta \quad (8)$$

where $\theta \in \mathbb{R}$ is spacelike and $(r, \chi) \in (\mathbb{R}^+ \times \mathbb{R}) \cup (\{\infty\} \times \mathbb{R}) \cup \{(0, 0)\}$ with r timelike and χ lightlike. As before, the boundaries are at $r = 0$ and $r = \infty$. This implies that the remaining compact direction on the boundary after unrolling θ is coordinatized by χ , which is lightlike. For future reference, note that this differs from the cover obtained by unwrapping the bulk with respect to the global t timelike direction instead of θ . The universal cover given by Eq. 8 is aligned with the σ Möbius twist along the θ direction and therefore undoes it. On the other hand, the cover that unwraps t does not contain the Möbius σ twist identification as a subgroup (i.e. t does not only wrap around the $r = 0$ part of the boundary like θ). While it still produces an orientable cover, we shall find that it differs on its boundary and will contain fixed points there.

Finally, for completeness we mention that the isometries of AdS_3 form the quotient group $\frac{\text{SL}(2, \mathbb{R}) \times \text{SL}(2, \mathbb{R})}{\mathbb{Z}_2}$. As discussed in the previous section, as a group manifold, AdS_3 is $\text{SL}(2, \mathbb{R})$. There are three (orientable) double covers possible for AdS_3 (and NO- AdS_3): the diagonal $\text{SL}(2, \mathbb{R}) \times \text{SL}(2, \mathbb{R})$, and the two off-diagonal $\frac{\text{Mp}(2, \mathbb{R}) \times \text{SL}(2, \mathbb{R})}{\mathbb{Z}_2}$ and $\frac{\text{SL}(2, \mathbb{R}) \times \text{Mp}(2, \mathbb{R})}{\mathbb{Z}_2}$ covers [41]. These last two differ by their chirality only. NO- AdS_3 's quotient isometry group corresponds to their quotient by $\sigma \equiv \mathbb{Z}_2$.

B. The Boundary of NO- AdS_3

The boundary of NO- AdS_3 is orientable despite the non-orientability of its bulk [41]. Non-orientability is a global topological property, and so is not locally identifiable. As a result, the isometries of the bulk of non-orientable AdS_3 are the same as for the orientable case: $\mathfrak{sl}(2, \mathbb{R}) \oplus \mathfrak{sl}(2, \mathbb{R})$.

On the other hand, the σ identification reduces the number of Killing vectors down to four at the boundary $\rho \rightarrow \infty$:

$$\chi_0 = \partial_{\omega_+}, \quad (9)$$

$$\chi_1^+ = \exp(i\omega_+) \partial_{\omega_+}, \quad (10)$$

$$\chi_{-1}^+ = \exp(-i\omega_+) \partial_{\omega_+}, \quad (11)$$

$$\chi_1^- - \chi_{-1}^- = \sin(\omega_-) \partial_{\omega_-}, \quad (12)$$

where $\omega_{\pm} \equiv \phi \pm t$ in terms of global coordinates. These are further reduced to just three at $\omega_- = 0, \pm\pi$, generating $\mathfrak{sl}(2, \mathbb{R})$.

In global AdS_3 coordinates, we showed how the σ identifies one AdS_3 with another with $(\ell, \rho, t, \phi) \rightarrow (i\ell, \rho + i\pi/2, \phi + \pi, t + \pi)$, where the transformation in t and ϕ can be equivalently expressed as $\sigma(\omega_+, \omega_-) = (\omega_+, -\omega_-)$.

The Wick rotation $\ell \rightarrow i\ell$ and transformation $\rho \rightarrow \rho + i\pi/2$ can be equivalently represented as $\rho \rightarrow \text{arcsinh}(\cosh(\rho))$ with ℓ fixed in the embedded coordinates, if their relationship to embedding coordinates is dropped. Either way, it follows that σ exhibits ‘‘fixed points’’ on the $\rho \rightarrow \infty$ boundary at the lines $\omega_- = 0$ and $\omega_- = \pm\pi$, precisely where the isometries reduce to $\mathfrak{sl}(2, \mathbb{R})$. The manifold is smooth at these fixed points and the Ricci scalar remains constant. However, as we shall see later, they must be excised in order to support a CFT_2 [42].

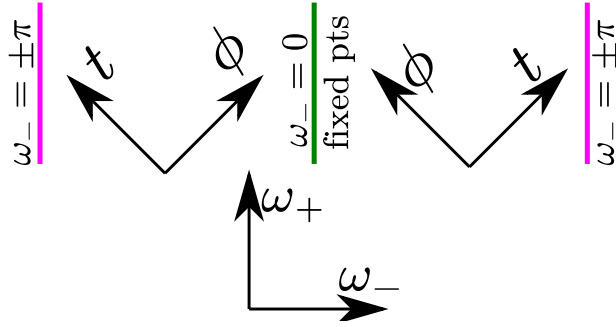


FIG. 3. The two-dimensional boundary of the orientable double cover of NO-AdS₃ consists of two sections separated by fixed points along $t - \phi = \omega_- = 0, \pm\pi$ with ∂_{ω_-} flipped on the two sides. This can be described as two boundaries with opposite spacetime orientation, which are not causally connected because the timelike Killing vector vanishes on the fixed lines that separate them. Note that the situation is the same for its (non-orientable) single cover because the boundary is actually still orientable.

The two fixed lines divide the boundary into two sections, $-\pi < \omega_- < 0$ and $0 < \omega_- < \pi$, which are the same except for being oppositely oriented with respect to each other. Specifically, the ∂_{ω_+} null basis vector is the same in both boundary sections while the other, $\sin(\omega_-)\partial_{\omega_-}$, flips: $\partial_{\omega_-} \leftrightarrow -\partial_{\omega_-} \Leftrightarrow t \leftrightarrow \phi$ (see Figure 3).

From this perspective, due to the flip in the Killing vector between these two strips, this boundary can be equivalently described as two orientations of the same strip. Heuristically, this implies that the two strips can be thought of as the “two sides” of a two-sided (i.e. orientable) strip; the coordinates on one strip are repeated in the second strip, but with opposite relative orientation. As a result, from this perspective, the boundary is neither exterior nor interior to the bulk. This can actually be seen as the consequence of the boundary of NO-AdS₃’s torus topology, which is geometrically equivalent to an orientable double cover of a Klein bottle; the cylindrical direction lies along the strips and the double cover of the Mobius strip is the perpendicular direction that cuts through both strips before coming back to itself; the fixed lines correspond to a twist and untwist (see Appendix A for more details).

A similar boundary can be found in self-dual AdS₃ [42, 43], which is a \mathbb{Z} quotient of one $SL(2, \mathbb{R})$ chiral side of the $SL(2, \mathbb{R}) \times SL(2, \mathbb{R})$ isometries of AdS₃. Two lines on the boundary can be similarly found to consist of fixed points of the \mathbb{Z} quotient. In both cases, this

means that if the appropriate timelike coordinate is unrolled, then the remaining compact cylindrical direction on the boundary is lightlike, unlike for AdS_3 where it is spacelike.

There is an important difference between non-orientable AdS_3 and the self-dual AdS_3 . In both cases, t and ϕ are bulk timelike and spacelike coordinates, and become lightlike on the boundary. However, for the self-dual AdS_3 the fixed lines on the boundary lie on null lines on the conformal boundary [42], while for non-orientable AdS_3 , $\omega_- = 0$, π lie along timelike lines corresponding to $r = 0$ in the Iwasawa metric (the remaining term when $r \rightarrow 0$ is timelike θ in Eq. A25-A26 in Appendix A). As a result, in self-dual AdS_3 a null coordinate lies along the strips and across the strips [42], while in NO- AdS_3 a timelike coordinate lies along the strips and a spacelike coordinate lies across the strips.

We will shortly be interested in an (orientable) infinite cover of NO- AdS_3 obtained by unwinding its bulk timelike dimension (specifically t in the usual global coordinates) so as to compare to the universal cover of AdS_3 . This infinite cover of NO- AdS_3 is orientable and removes closed timelike curves. However, the Mobius “twist” in NO- AdS_3 is along its null θ direction. This means that this infinite cover of NO- AdS_3 continues to differ on its boundary from AdS_3 .

Notably, as mentioned at the end of Section II A, the fixed lines remain present on the boundary of the orientable infinite cover of NO- AdS_3 , since the cover does not contain the $\sigma \equiv \mathbb{Z}_2$ as a subgroup. Specifically, since $\omega_- = 0$, $\pm\pi$ is timelike on the boundary of the single cover, the boundary of this infinite cover of NO- AdS_3 contains fixed points along its boundary spacelike dimension, $\phi = 0, \pm\pi$, too (see Fig. 4).

As a result, the bulk metric of this orientable infinite cover of NO- AdS_3 asymptotes to two boundary strips that are oppositely oriented and run up and down in the bulk timelike direction. This allows for the possibility of defining a pair of antipodal Rindler wedges so that their boundaries overlap with distinct boundary strips. As we shall see in the next section, this set-up simplifies the analysis of the relationship between the bulk and boundary in NO- AdS_3 .

C. Holography of NO- AdS_3

Non-orientable AdS_3 's bulk classical theory can be captured by the purely topological three-dimensional Chern-Simons gauge theory with $\text{SL}(2, \mathbb{R}) \times \text{SL}(2, \mathbb{R})$ gauge, where the

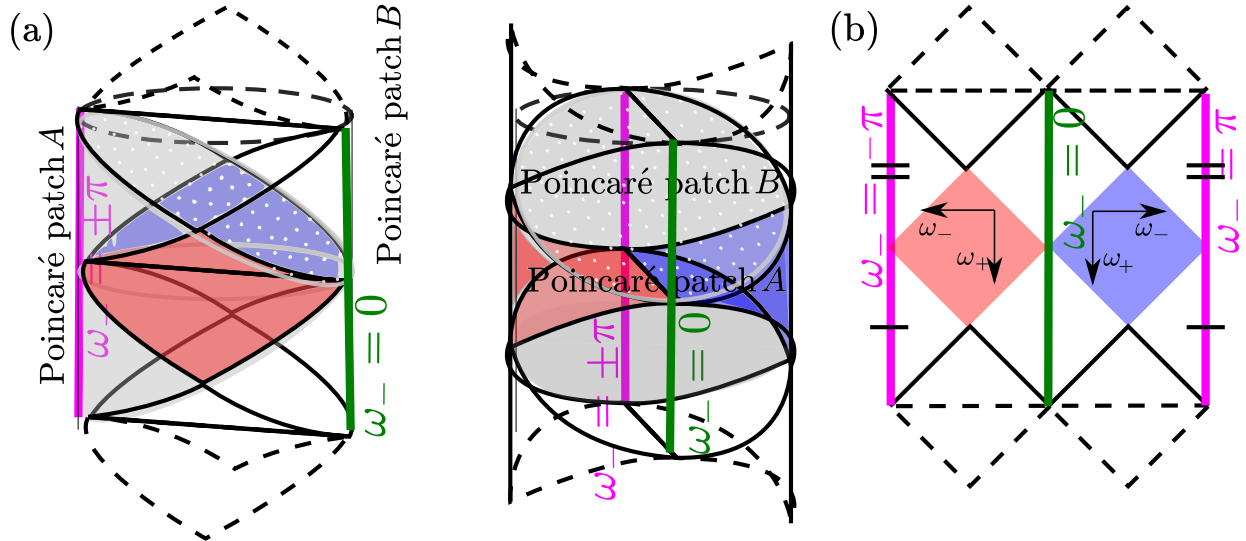


FIG. 4. (a) Two perspectives of the (orientable) infinite cover of NO-AdS₃ from unrolling global timelike t , which are rotated by $\frac{\pi}{2}$ with respect to each other. A Rindler patch and its antipode are colored red and blue, respectively. b) Antipodal Rindler patches can be fully contained within each Poincaré patch where their boundaries coincide with different strips. This infinite cover of NO-AdS₃ still contains the single cover's fixed lines (pink and green), unlike the universal cover of AdS₃, due to being an unrolling in the bulk t direction compared to NO-AdS₃'s twist, which is along the bulk θ direction.

action of each chiral $SL(2, \mathbb{R})$ is equal to the other (multiplied by -1), unlike for orientable AdS₃ [41, 44]. As a result, the theory becomes a two-dimensional WZW model on its boundary defined by chiral $SL(2, \mathbb{R})$ factors that have opposite signs. Here we will first show that its AdS₃/CFT₂ correspondence implies a similar dual boundary theory based on two oppositely oriented boundary conformal field theories (BCFTs). We will then show that the AdS₃/BCFT₂ correspondence implies a similar bulk theory to the Chern-Simons gauge theory in terms of a pair of end-of-the-world Dirichlet-branes.

As noted in the prior section, the boundary of NO-AdS₃ is actually orientable, where each strip is oppositely oriented to the other delineated by a shared pair of lines consisting

of fixed points. Despite the smoothness of the manifold, fixed points must be excised in order for a manifold to support a CFT₂ [42], at which point they define a co-dimension one boundary on the boundary itself. Following Cardy [45], after excising the fixed lines, the algebra of the conformal two-dimensional manifold corresponding to each strip is reduced to a single chiral copy because the holomorphic or antiholomorphic fields that generate the pair of chiral algebras are not independent of each other at the boundary lines (i.e. they have shared boundary conditions).

In particular, for a free boson $X(\sigma, \tau)$ with spacelike σ and timelike τ and action

$$S = \frac{1}{4\pi} \int d\sigma d\tau ((\partial_\sigma X)^2 + (\partial_\tau X)^2), \quad (13)$$

variation of the action δS produces the boundary term

$$\frac{1}{\pi} \int_B dl_B (\vec{\nabla} X \cdot \vec{n}) \delta X. \quad (14)$$

Specific boundary conditions determine how each copy depends on the other. Imposing Dirichlet boundary conditions along the timelike boundary at $\sigma = 0$ by setting $\delta X|_{\sigma=0} = 0 \Leftrightarrow \partial_\tau X|_{\sigma=0} = 0$, results in $j_n = -\bar{j}_n$, where the j_n are the n th Laurent modes of $j(z) = i\partial X(z, \bar{z})$. This aligns with the boundary WZW model where each chiral $\text{SL}(2, \mathbb{R})$ has the opposite sign compared to the other.

This contrasts with the boundary theory of self-dual AdS_3 whose fixed points lie along a null manifold $\sigma - \tau = 0, \pi$ (i.e. the boundary is rotated by $\pi/4$) [42, 46]. With such a boundary, Neumann or Dirichlet boundary conditions correspond to $\partial_{\sigma \pm \tau} X|_{\sigma - \tau = 0} = 0$, which set either $j_n = 0$ or $\bar{j}_n = 0$. As a result, chiral AdS_3 's boundary theory consists of two chiral CFT₂s with one having zero central charge [47, 48].

In NO- AdS_3 the two strips on the boundary corresponding to $0 < \omega_- < \pi$ and $\pi < \omega_- < 2\pi$, share the same boundary conditions, albeit with flipped orientations. This means each strip can support a BCFT₂, which produces a direct sum of two Hilbert spaces corresponding to opposite orientations of the same space, where each supports a state $|\Omega\rangle$ and $|\bar{\Omega}\rangle$, respectively, corresponding to a Cardy boundary (ground) states,

$$|\Omega\rangle = \sum_h \sum_N \sum_j^{\infty} d_h(N) B_h |h, N; j\rangle \otimes U |\bar{h}, \bar{N}; \bar{j}\rangle, \quad (15)$$

and

$$|\bar{\Omega}\rangle = \sum_h \sum_N \sum_j^{\infty} d_h(N) (B_h)^* |\bar{h}, \bar{N}; \bar{j}\rangle \otimes U |h, N; j\rangle. \quad (16)$$

$\sum_j |h, N; j\rangle \otimes U |\bar{h}, \bar{N}; \bar{j}\rangle$ is an Ishibashi basis state with weight h and level N , B_j is determined by the boundary conditions [49], and the unitary $U = I$ for diagonal CFTs.

Since the excised fixed lines at their boundaries prevent trajectories on one side from getting to the other and becoming causally dependent, the full two-dimensional boundary space supports $|\Omega\rangle \otimes |\bar{\Omega}\rangle \equiv |\Omega\rangle |\bar{\Omega}\rangle$. As we shall find in Section IID, taking the orientable infinite cover of this space (along the bulk t timelike direction) changes the identification of $|\Omega\rangle$ and $|\bar{\Omega}\rangle$ to correspond to boundary conditions that are infinitely separated, but does not change the trivial product decomposition of $|\Omega\rangle |\bar{\Omega}\rangle$.

As first noted in the previous section, a bulk Rindler wedge (and its antipode) can be defined such that its boundary overlaps with only one strip (and the opposite strip; see Fig. 4). It is well-known that a Rindler wedge corresponds to the bulk region that is causally connected to its boundary causal diamond. Redefining the state $|\Omega\rangle$ to be restricted only on the boundary of a Rindler wedge, and $|\bar{\Omega}\rangle$ to be restricted on the boundary of its opposite orientation, each $|\Omega\rangle$ and $|\bar{\Omega}\rangle$ state can be considered to correspond to an open string restricted to the Rindler wedge's boundary.

A Rindler wedge (red in Fig. 4) and its antipodal counterpart (blue in Fig. 4) are connected in NO-AdS₃ by closed timelike curves. Taking the orientable infinite cover of NO-AdS₃ by unwinding the t dimension removes these closed curves so that antipodal Rindler wedges (e.g. red and blue) are no longer timelike separated. Importantly, the boundary fixed lines remain present.

As a result, in this infinite cover of NO-AdS₃, a Rindler wedge and its antipode's boundaries continue to overlap with different strips after they are no longer connected by closed timelike loops. This means that they are now purely spacelike separated, but also that their bulks asymptote to oppositely oriented boundaries, which support unentangled Hilbert spaces. We proceed to study the effect of these distinct asymptotic regions in the bulk Rindler states using the framework of the AdS/BCFT duality, where the bulk dual of a single strip of the boundary CFT, say between $\omega_- \in (0, \pi)$, can be found by evaluating the gravitational path integral with an end-of-the-world (EOW) brane through the bulk [50]. We will find that the symmetry of the CFT boundary conditions results in a tensionless geodesic brane through the diameter of AdS.

Let \mathcal{M} denote the bulk dual manifold whose boundary consists of an asymptotic component, denoted \mathcal{B} , and a brane component, denoted Q , so that $\partial\mathcal{M} = \mathcal{B} \cup Q$. The brane

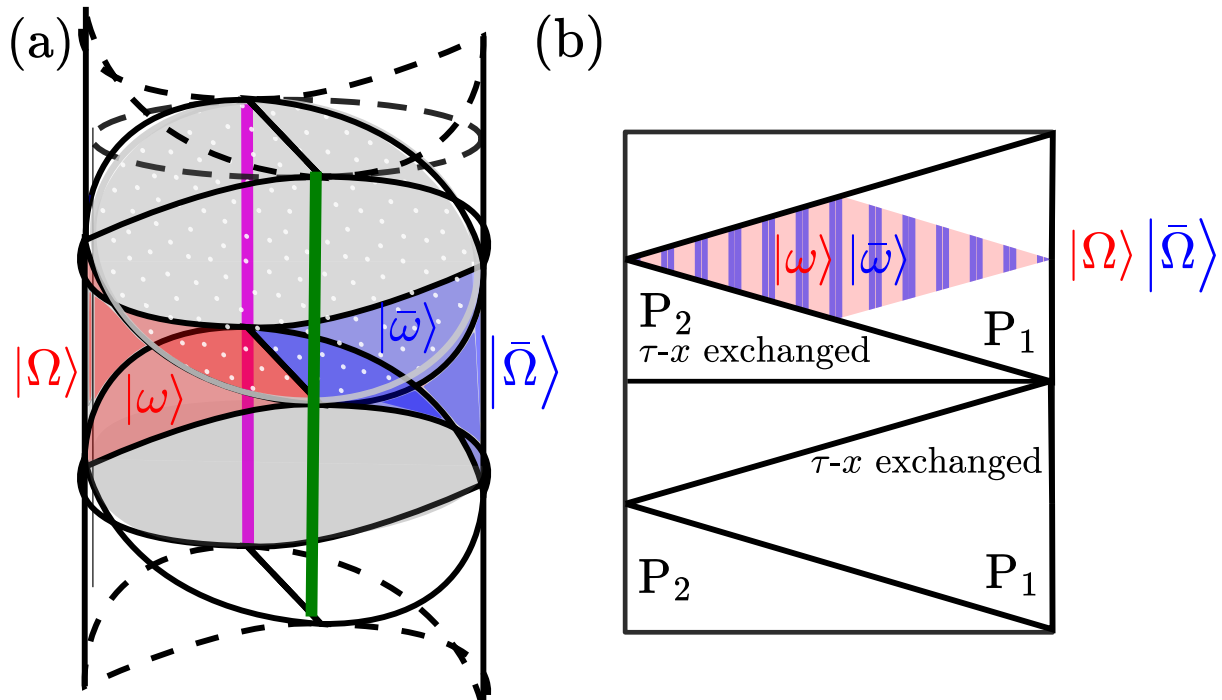


FIG. 5. (a) The orientable infinite cover of NO-AdS₃ with unwrapped t with annotated boundary $|\omega\rangle$, $|\bar{\omega}\rangle$ and corresponding bulk $|\Omega\rangle$, $|\bar{\Omega}\rangle$ states, respectively. (b) The Penrose diagram of the orientable double cover of NO-AdS₃. The blue and red diamonds show the conformal projection of the two antipodal Rindler patches in Poincaré patch P_1 shown in Fig. 4 (note that these Rindler patches do not “fill out” the dropped dimensions at most points; one Rindler patch is “in front” of the other). $|\omega\rangle$ and $|\bar{\omega}\rangle$ are bulk states defined on antipodal Rindler patches with boundary dual states $|\Omega\rangle$ and $|\bar{\Omega}\rangle$, respectively.

obeys a homology constraint, such that its boundary coincides with the boundary of \mathcal{B} , i.e. with the fixed lines on $\partial\mathcal{M}$. Denoting the lines (upon which Dirichlet conditions are imposed) by D_0 and D_π , this means that $\partial Q = \partial\mathcal{B} = D_0 \cup D_\pi$. The EOW brane is found via the saddle-point approximation to the gravitational path integral, e.g. by extremizing the Einstein-Hilbert action

$$S = \frac{1}{16\pi G_N} \int_{\mathcal{M}} \sqrt{-g}(R - 2\Lambda) + \frac{1}{8\pi G_N} \int_{\partial\mathcal{B}} \sqrt{-h}K + \frac{1}{8\pi G_N} \int_Q \sqrt{-h}(K - T) \quad (17)$$

where we have assumed that the matter contribution to the brane action is due solely to tension T , i.e. $T_{ab}^{matter} = Th_{ab}$. The brane equation of motion is well-known:

$$K_{ab} - \frac{1}{2}Kh_{ab} = -8\pi G_N Th_{ab} \quad (18)$$

where K_{ab} is the extrinsic curvature of Q and h_{ab} is the induced metric on Q .

Taking our ansatz bulk geometry to be that of NO-AdS₃, or equivalently AdS₃ (these geometries can be locally identified within a single Poincare patch), it can be straightforwardly verified that, in global coordinates, the brane is parameterized by

$$\sinh \rho \sin \phi = \sinh \rho_* \quad (19)$$

where the ρ_* is related to the brane tension via

$$T = \frac{1}{L} \tanh \rho_* \quad (20)$$

specifically, the range of ϕ is covered by two branches:

$$\phi(\rho) = \begin{cases} \sin^{-1} \left(\frac{\sinh \rho_*}{\sinh \rho} \right), & \rho \in (\rho_*, \infty) \\ \pi - \sin^{-1} \left(\frac{\sinh \rho_*}{\sinh \rho} \right), & \rho \in (\rho_*, \infty) \end{cases} \quad (21)$$

Since completely reflecting (i.e. Dirichlet) conditions on D_0 and D_π are necessary to ensure the factorization of the CFT vacuum, and since $D_0 \cup D_\pi = \partial Q$, this suggests that Dirichlet conditions must be imposed on the entirety of Q . This suggests that we take the tensionless limit, i.e. $\rho_* \rightarrow 0$, resulting in a timelike brane that bisects AdS₃:

$$\phi(\rho) = \begin{cases} 0, & \rho \in (0, \infty) \\ \pi, & \rho \in (0, \infty) \end{cases} \quad (22)$$

This brane intersects every constant time slice $t = t_0$ at precisely the edge of the bulk domain of dependence of the boundary $t = t_0$ slice between D_0 and D_π . That is, on the $t = t_0$ slice, it coincides with the bifurcate Rindler horizon of the region dual to the t_0 slice of the BCFT.

Since the bulk dual to the CFT supported on the $\omega_- \in (0, \pi)$ terminates at the brane, this immediately implies that the bulk vacuum is supported on Cauchy slices which terminate at the brane. Consequently, the vacuum is supported on a single Rindler wedge. In particular, if the state $|\Omega\rangle$ is supported on region $\omega_+ = 0, \omega_- \in (0, \pi)$, then its bulk dual is a pure state $|\omega\rangle$ supported on corresponding Rindler wedge.

However, our BCFT does not consist solely of a single CFT in the region $\omega \in (0, \pi)$. A second non-interacting copy lives on the $\omega \in (-\pi, 0)$ region. One finds an identical set

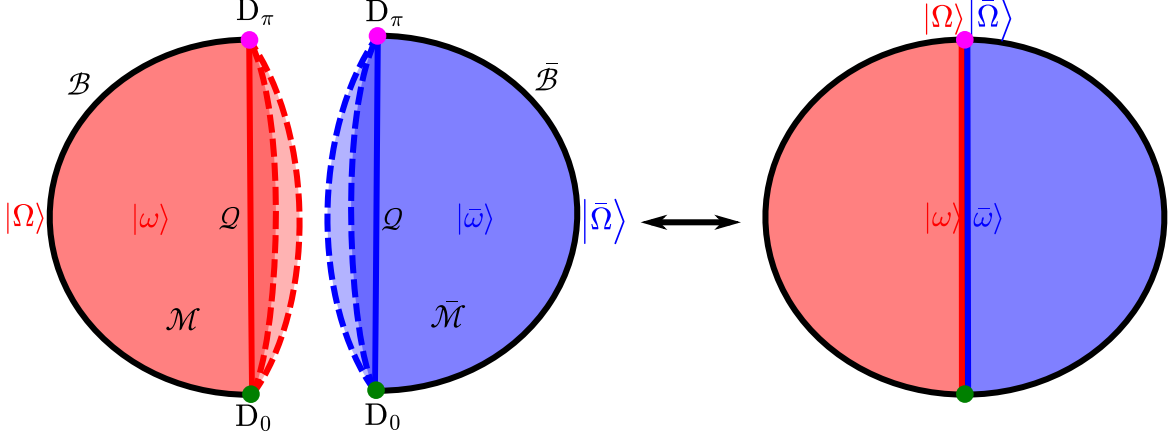


FIG. 6. On the left are timeslices of the bulk regions dual to the BCFT's defined on \mathcal{B} and $\bar{\mathcal{B}}$. The dashed lines depict brane solutions of Eq. 18 with nonvanishing tension. The solid lines depict the tensionless branes. In the tensionless limit with Dirichlet conditions on the branes, the two bulk regions can be regarded as glued along their shared boundaries.

of bulk branes, and in the tensionless limit, the brane coincides with the bisecting brane discussed above. Likewise, the BCFT state $|\bar{\Omega}\rangle$ supported on $\omega_+ = 0, \omega_- \in (-\pi, 0)$ is dual to a bulk state $|\bar{\omega}\rangle$ supported on the Rindler wedge antipodal to that supporting $|\omega\rangle$. In particular, the bulk dual to the BCFT product state $|\Omega\rangle |\bar{\Omega}\rangle$ is the state $|\omega\rangle |\bar{\omega}\rangle$ supported on antipodal Rindler wedges. The lack of entanglement in the bulk vacuum is a consequence of the Dirichlet boundary conditions imposed on the bisecting brane.

Finally, note that although we have performed the brane calculation for each BCFT half separately, since the boundary conditions are symmetric, we could regard them as living on two halves of a shared manifold, which is glued along the brane. In particular, the Dirichlet conditions on the shared BCFT boundary $D_0 \cup D_\pi$ ensures that we can equivalently regard the two CFT's as either living on two halves of a single CFT manifold with Dirichlet conditions imposed on the surface $D_0 \cup D_\pi$, or as two "disconnected" CFTs supported on half spaces \mathcal{B} and $\bar{\mathcal{B}}$ each ending at $\partial\bar{\mathcal{B}} = \partial\mathcal{B}$, with bulk duals \mathcal{M} and $\bar{\mathcal{M}}$ each ending on Q , and which are subsequently glued along their boundaries. This is depicted in Fig. 6

To summarize, the state $|\omega\rangle$ (or $|\bar{\omega}\rangle$) corresponds e.g. to the red (blue) bulk Rindler wedges in (a) of the orientable infinite cover depicted in Fig. 4, and $|\Omega\rangle$ (or $|\bar{\Omega}\rangle$) corresponds to state on the the red (blue) boundary diamonds depicted in (b) of the same figure. Furthermore, since a pair of Rindler patches contains a global spatial slice of the full NO-AdS₃ spacetime, $|\omega\rangle |\bar{\omega}\rangle$ must correspond to a bulk vacuum state of the orientable infinite cover of NO-AdS₃,

which is dual to the CFT_2 ground state $|\Omega\rangle|\bar{\Omega}\rangle$.

D. Instability of NO-AdS₃ to Quantum Gravity Dynamics

The two fixed lines (i.e. boundary conditions) in NO-AdS₃ have a finite proper distance between them before t is unwrapped. This means that in the corresponding two-dimensional conformal manifolds, where these fixed lines are excised, the length between them is finite in the NO-AdS₃ target space.

As previously discussed, ω_- becomes spacelike (and so ω_+ becomes timelike) on the boundary of NO-AdS₃. As a result, when t is unwrapped to produce an orientable infinite cover of NO-AdS₃, only ω_+ is unwrapped on the boundary (see Fig. 7). However, since unwrapping one dimension of a CFT_2 with boundary is conformally equivalent to unwrapping both dimensions (see Fig. 7d), unwrapping ω_+ also elongates the finite proper distance in ω_- between the fixed lines in the NO-AdS₃ target space to infinity.

As a result, unwrapping t separates the boundary conditions so that the proper distance between a fixed point line $\omega_- = 0$ and the former $\omega_- = \pm\pi$ becomes infinite and the corresponding open string length $\alpha \rightarrow \infty$. The Cardy formula,

$$\rho(L_0) \sim e^{2\pi\sqrt{\frac{cL_0}{6}}}, \quad (23)$$

reveals that for bosonic string excitations at level n with $m^2 \sim E \sim n/\alpha$, we have $\rho(E) \sim \exp(\tilde{c}E\sqrt{\alpha})$. With $T = (\frac{\partial S}{\partial E})^{-1}$, the Hagedorn temperature becomes $T_H \sim \alpha^{-1/2} \rightarrow 0$ [51]. Hence, this CFT_2 has vanishing Hagedorn temperature and is unstable to all excitation above the vacuum state.

A similar instability can be found for AdS₂ and self-dual AdS₃ as a consequence of the null energy condition [46]. Long strings have been studied in these contexts [40].

E. NO-(AdS₃ × S²) Construction

To study the global vacuum of the dS₄ fiber bundle in the next section, we will use a conformal map between its static patches, and Rindler wedges of NO-(AdS₃ × S²). We take a brief detour to introduce this larger fibered space of non-orientable AdS₃.

Recall that AdS₃ can be represented as an embedded surface in $\mathbb{R}^{2,2}$ as either $-u^2 - v^2 + x^2 + y^2 = -\epsilon$ or $-u^2 - v^2 + x^2 + y^2 = \epsilon$, with $\epsilon > 0$, and these two constraint equations are

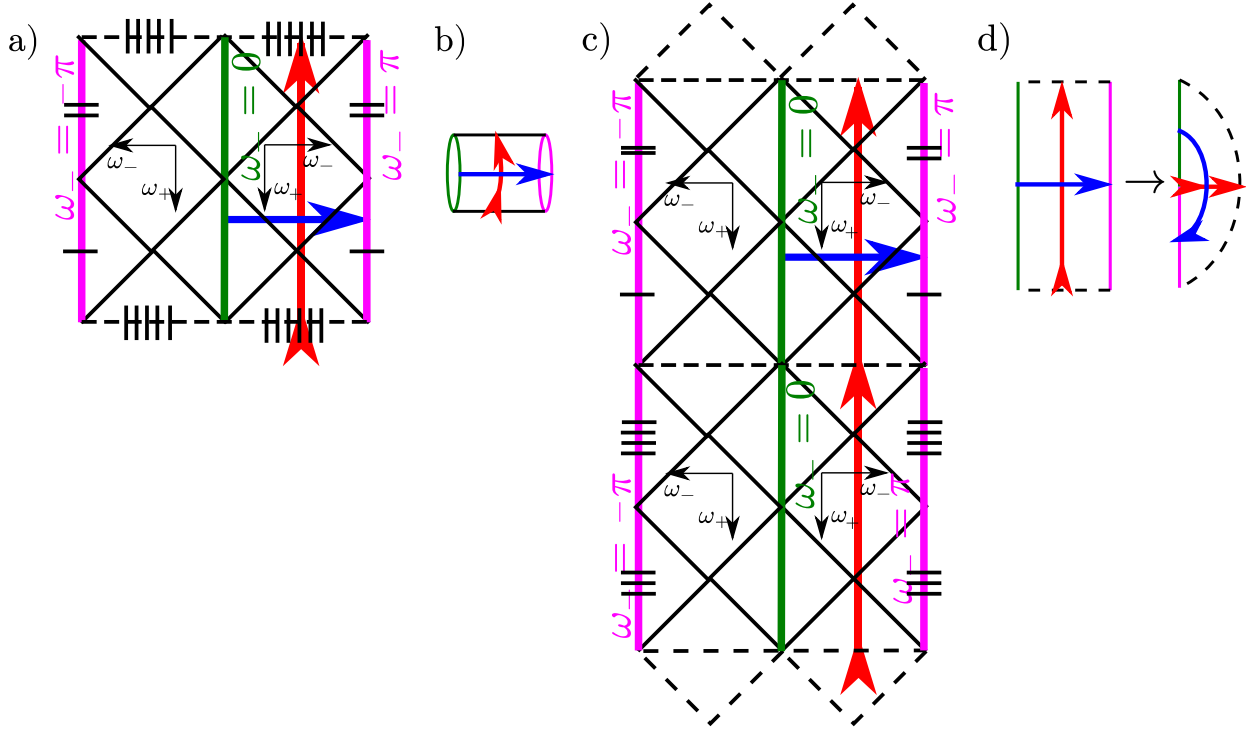


FIG. 7. a) The (single cover of the orientable) boundary of NO-AdS₃ is shown with periodic spatial direction (red arrow) and finite-length timelike direction (blue arrow). These can be considered as supporting a finite-length open string (blue) and closed string (red), respectively. b) This means that each strip is equivalent to a cylinder topology with a finite width. c) The infinite cover with respect to t unwraps the boundary's periodic timelike (red) direction. The remaining compact direction is lightlike instead of spacelike, unlike in the universal cover of AdS₃. d) Unwrapping makes each strip topologically equivalent to an infinite strip. Since this is conformally equivalent to the half-plane, it is the worldsheet of an open string (blue) or closed string (red) extending to infinite length.

related to one-another by the map $\sigma(u, v, x, t) = -(x, y, u, v)$. This relationship was used to construct NO-AdS₃ via a quotient of a double cover of AdS₃ by the map σ . To construct a non-orientable NO-(AdS₃ × S²), we similarly observe that AdS₃ × S² may be embedded into an $\mathbb{R}^{2,5}$ lightcone via the following constraint equations:

$$\underbrace{-u^2 - v^2 + x^2 + y^2}_{=-\epsilon} + \underbrace{a^2 + b^2 + c^2}_{=+\epsilon} = 0. \quad (24)$$

As in the three-dimensional case, an opposite signature AdS₃ can be embedded into a par-

tially Wick-rotated lightcone by changing the sign of ϵ in the embedding equations:

$$\underbrace{-u^2 - v^2 + x^2 + y^2}_{=+\epsilon} + \underbrace{a^2 + b^2 + c^2}_{=-\epsilon} = 0. \quad (25)$$

These constraints are related to the previous ones by simultaneously performing $\sigma(u, v, x, y) = -(x, y, u, v)$ along with a Wick rotation of the (a, b, c) coordinates. By constructing an appropriate double cover of the $\mathbb{R}^{2,5}$ lightcone, and quotienting by a map which simultaneously exchanges the AdS_3 coordinates and Wick rotates the S^2 coordinates, we can obtain a non-orientable fiber bundle space, $(\text{NO}-(\text{AdS}_3 \times S^2), \text{AdS}_3, \pi, S^2)$, such that the continuous surjective map $\pi : \text{NO}-(\text{AdS}_3 \times S^2) \rightarrow \text{NO-AdS}_3$ behaves like a projection from the corresponding regions of $\text{AdS}_3 \times S^2 \rightarrow \text{AdS}_3$ on each Poincaré patch, which we denote by $\text{NO}-(\text{AdS}_3 \times S^2)$. See Appendix B for more details.

Compared to NO-AdS_3 , the two glued Poincaré patches are augmented by S^2 product spaces: the $y > 0$ patch is accompanied by an S^2 space while the $y < 0$ patch (with exchanged τ and x) is accompanied by an oppositely oriented S^2 space. The resultant metric is

$$ds^2 = \begin{cases} \frac{1}{y^2} (-d\tau^2 + dx^2 + \epsilon dy^2) + \epsilon d\Omega_2^2, & y > 0, \\ \frac{1}{y^2} (-dx^2 + d\tau^2 + \epsilon dy^2) + \epsilon d\bar{\Omega}_2^2, & y < 0, \end{cases} \quad (26)$$

where the S^2 factor with metric $d\bar{\Omega}_2^2$ is antipodally parameterized by $(\pi - \theta, 2\pi - \phi)$. Therefore, we see that the S^2 appears as a non-trivial fiber, rather than as a separate, non-orientable factor.

The only new aspect of the $\text{NO}-(\text{AdS}_3 \times S^2)$ topology (compared to just non-orientable AdS_3) is the non-trivial fibering of the S^2 factor. However, this does not make the spacetime non-orientable in this factor; a path that completes a 2π loop in non-spacetime-orientable AdS_3 necessarily finds that its dimensions in the S^2 factor have returned to their original orientation due to the fibering. This can be seen in the Penrose diagram of the orientable double cover of $\text{NO}-(\text{AdS}_3 \times S^2)$ (see Fig. 8) where the sign of r (i.e. the orientation of the two-sphere) flips along with the sign of y and not with the $\tau - x$ exchange.

As a result of the added S^2 fiber, the structure of $|\omega\rangle$ and $|\bar{\omega}\rangle$ may change. However, given that the S^2 vanishes at the NO-AdS_3 boundary (i.e. $y \rightarrow 0$ makes the NO-AdS_3 metric infinitely larger than the S^2 in Eq. 26), the $|\Omega\rangle$ and $|\bar{\Omega}\rangle$ are expected to remain unchanged

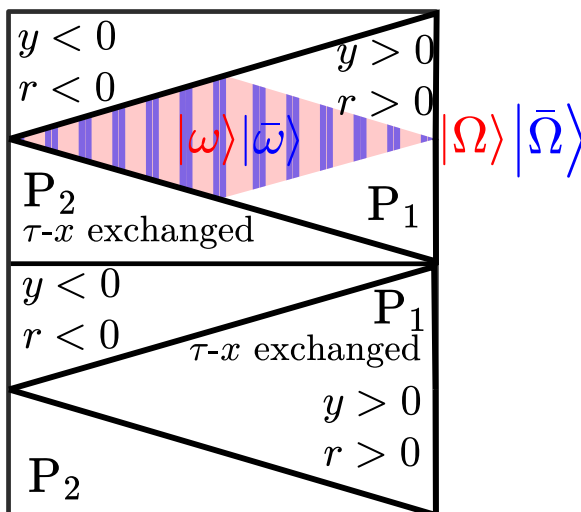


FIG. 8. The Penrose diagram of the orientable double cover of NO-(AdS₃ × S²). The blue and red diamonds show the projection of the two antipodal Rindler patches in Poincaré patch P₁ shown in Fig. 4 (note that these Rindler patches do not “fill out” the dropped dimensions at most points).

as Cardy states. Specifically, the Brown-Henneaux conditions for AdS₃ with global metric $ds^2 = -f(r)dt^2 + f^{-1}(r)dr^2 + r^2d\theta^2$ [52] are:

$$g_{AB} = r^2\gamma_{AB} + \mathcal{O}(1), \quad (27)$$

$$g_{rA} = \mathcal{O}(r^{-3}), \quad (28)$$

$$g_{rr} = \frac{\ell^2}{r^2} + \mathcal{O}(r^{-4}), \quad (29)$$

where γ_{AB} is a fixed metric on the cylinder at spatial infinity $r \rightarrow \infty$ and $x^A = (t, \theta)$. NO-(AdS₃ × S²) satisfies these conditions since the S² bundle can be considered to add as a $\mathcal{O}(r^{-2})$ factor in g_{AB} , which is contained in $\mathcal{O}(1)$.

Regardless, the holographic correspondence between bulk $|\omega\rangle$ and $|\bar{\omega}\rangle$ states and boundary $|\Omega\rangle$ and $|\bar{\Omega}\rangle$ states, respectively, remains the same (see Fig. 8).

III. OB-dS₄ × ℝ

In this section we will derive a de Sitter spacetime, with product space ℝ, and examine its properties within quantum gravity. We proceed with a derivation in Section III A. We will examine the oppositely oriented boundaries of this spacetime and show their consequences

on the static patches. Otherwise, we show that the de Sitter spacetime shares the same boundary as regular dS_4 . Finally, in Section III B we discuss its bulk/boundary correspondence by utilizing a generalization of the conformal map between static patches of $dS_4 \times \mathbb{R}$ and Rindler wedges of the universal cover of $AdS_3 \times S^2$.

A. OB- $dS_4 \times \mathbb{R}$ Construction

Consider the $\mathbb{R}^{2,5}$ lightcone used in the construction of NO- $(AdS_3 \times S^2)$. Rather than embedding $AdS_3 \times S^2$ via the restrictions given by Eqs. 24-25, we instead impose $dS_4 \times \mathbb{R}$ restrictions via the following constraint equation:

$$\underbrace{-u^2 + x^2 + a^2 + b^2 + c^2}_{=+\epsilon} \underbrace{-v^2 + y^2}_{=-\epsilon} = 0. \quad (30)$$

We do not expect σ to be a subgroup of the bulk isometries of $dS_4 \times \mathbb{R}$ or its higher covers. This is easy to verify by noting that it cannot be expressed in global coordinates of $dS_4 \times \mathbb{R}$ (see Appendix C).

However, it can be found to be expressible in terms of Poincaré coordinates of $dS_4 \times \mathbb{R}$. In fact, we shall find that σ should only be considered as producing orbifold spacetimes when considered over Poincaré patches (or subpatches thereof) of $dS_4 \times \mathbb{R}$. In other words, σ is a \mathbb{Z}_2 subgroup of a double cover (of a subgroup) of the bulk isometry group $SO^+(1, 3) \times \mathbb{R}$ of either pair of Poincaré patches of $dS_4 \times \mathbb{R}$ but not of the bulk isometry group $SO^+(1, 4) \times \mathbb{R}$ of global $dS_4 \times \mathbb{R}$ (or any higher covers). Specifically, we shall find that σ does not preserve the $SO(4)$ isometry of the S^3 of dS_4 's global topology, but does preserve the local $SO(3)$ isometries of the S^2 's fiber bundle over S^1 that makes up S^3 . Poincaré patches only contain the S^2 's on half of the S^1 , and so contain the σ as a subgroup of a double cover of their bulk isometries. Therefore, there is only a meaningful orbifold formed when taking a quotient of Poincaré patches of $dS_4 \times \mathbb{R}$ (or subpatches thereof).

Let us specifically consider flat slicing coordinates on $u+x > 0$ where the $u = \ell \sinh(t/\ell) + \frac{r^2 e^{t/\ell}}{2\ell}$, $x = \ell \cosh(t/\ell) - \frac{r^2 e^{t/\ell}}{2\ell}$, and $a = e^{t/\ell} y_i$ etc., for $r^2 = \sum_i y_i^2$, and hyperbolic coordinates for \mathbb{R} : $v = \ell \cosh(\phi)$ and $y = \ell \sinh(\phi)$. The time coordinate in Poincaré coordinates corresponds to $\eta = \eta_{t=\infty} - \ell e^{t/\ell}$. Projected onto the embedded manifold's coordinates, σ

can be expressed by

$$\ell \rightarrow i\ell, t \rightarrow it - \frac{\pi}{2}\ell, \phi \rightarrow \phi + i\frac{\pi}{2}, y_i \rightarrow y_i. \quad (31)$$

Choosing instead the other Poincaré patch with the same spacelike boundary involves taking $x \rightarrow -x$ and so requires changing σ 's definition to

$$\ell \rightarrow -i\ell, t \rightarrow -it + \frac{\pi}{2}\ell, \phi \rightarrow \phi - i\frac{\pi}{2}, y_i \rightarrow y_i. \quad (32)$$

The expanding Poincaré patch with $u + x > 0$ and the other expanding Poincaré patch with $u - x > 0$ are partially overlapping. Quotienting by σ independently preserves a subgroup of each patch's isometry group. However, the resultant two spaces are no longer covers of the same global space and should be considered to be two different quotients of the same $dS_4 \times \mathbb{R}$ spacetime that splits it up into two different pairs of spaces.

Another way to see this is by noting that when σ is projected onto embedded Poincaré coordinates it introduces fixed points along their Poincaré horizons. Since σ is not a subgroup of the global isometry group of $dS_4 \times \mathbb{R}$, these fixed points actually correspond to points of geodesic incompleteness, i.e. singularities. Singularities cannot be observer-dependent. Specifically, we can find from Eqs. 31-32 that σ introduces fixed points at $t/\ell \rightarrow \pm\infty$, $\phi \rightarrow \pm\infty$. Since the “extra” fifth dimension coordinatized by ϕ is conformally suppressed by η at the Poincaré spacetime boundaries, only the $t/\ell \rightarrow -\infty$, $\phi \rightarrow \pm\infty$ fixed points are reachable. This corresponds to a lightlike singularity on the Poincaré horizon at $\phi = \pm\infty$. This is true of either pair of contracting and expanding Poincaré patches of the spacetime (see Fig. 9). Since the Poincaré horizon contains “naked” singular points, in order to have well-defined Hamiltonian evolution from past Cauchy slices, we place Dirichlet conditions along the entire Poincaré horizon. This is also compatible with the change in the orientation of the S^2 at the Poincaré horizon.

As a result, it is not possible to express Eq. 31 in terms of the $u - x \leq 0$ Poincaré patches directly (i.e. without going through the embedding space) because it breaks up the $u - x \leq 0$ Poincaré patches along the former's singular Poincaré horizon. Similarly, Eq. 32 can be found to break up the $u + x \leq 0$ Poincaré patches. Therefore, though Eq. 31 and Eq. 32 can both be inferred from σ when it is expressed in embedding coordinates, it corresponds to multiple distinct operations in embedded coordinates, and produce different quotient spacetimes depending on which covering space of $dS_4 \times \mathbb{R}$ is initially considered.

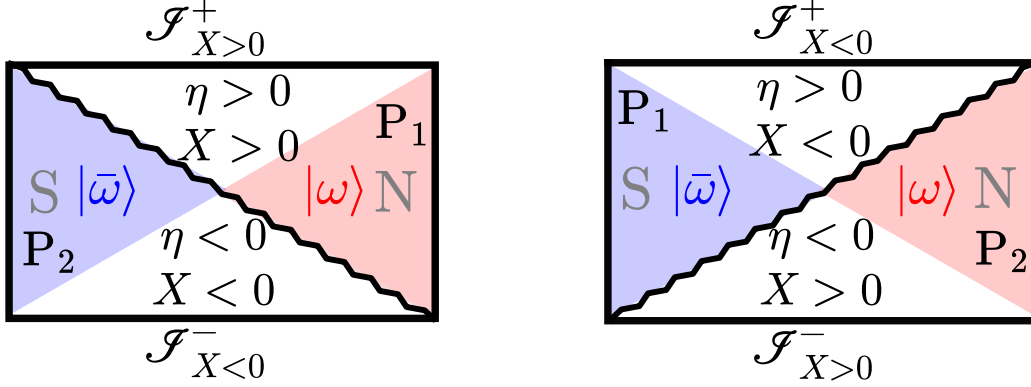


FIG. 9. Penrose diagram of two OB-dS₄ × ℝ quotient spacetimes, corresponding to Eq. 31 and Eq. 32, composed of expanding and contracting Poincaré patches. Regardless of which quotient spacetime is considered, antipodal static patches only experience one orientation of S³, e.g. the blue patch only sees X < 0 while the red patch only sees X > 0. A lightlike singularity exists at the horizons of the Poincaré patch.

Considering Eq. 30 along with its opposite constraint,

$$\underbrace{-u^2 + x^2 + a^2 + b^2 + c^2}_{=-\epsilon} \underbrace{-v^2 + y^2}_{=+\epsilon} = 0. \quad (33)$$

allows us to proceed in a similar manner to before to define this new spacetime (see Appendix D). The result is

$$ds^2 = \begin{cases} \frac{1}{\eta^2} (-d\eta^2 + dX^2 + X^2 d\Omega_2^2 + \eta^2 L^2 d\phi^2), & \eta > 0, X > 0, \phi \in \mathbb{R}, \\ \frac{1}{\eta^2} (-d\eta^2 + dX^2 + X^2 d\Omega_2^2 + \eta^2 L^2 d\phi^2), & \eta < 0, X < 0, \phi \in \mathbb{R}. \end{cases} \quad (34)$$

This metric describes two opposite Poincaré patches, i.e. the expanding region for $\eta > 0$ and the contracting region for $\eta < 0$, with oppositely oriented bulk S²s and parity-flipped fifth spatial dimensions, respectively. The opposite orientation of the S² factors is revealed by the fact that $X < 0$ in the second branch, although now this flips the orientation of the spatial S³, since $X \in \mathbb{R}$ and is not fixed. By this we mean that, in spherical coordinates, if the $X > 0$ portion of the S³ is coordinatized by (X, θ, ϕ) for $\theta \in (0, \pi)$, $\phi \in (0, 2\pi)$, then the $X < 0$ portion of the S³ coordinatized by (X, θ, ϕ) is equivalently described by $(X, \pi - \theta, 2\pi - \phi)$ with $X > 0$, and therefore has opposite orientation.

It is important to note that, unlike NO-(AdS₃ × S²), the oppositely oriented S²s appear *within* the dS₄ geometry, rather than as a non-trivial fiber attached to dS₄. Rather, it is the ℝ factor which is fibered with the OB-dS₄, but unlike the S², it appears as a trivial factor.

Finally, let us determine the bulk isometries of OB-dS₄ × ℝ. We can start with the bulk isometries of dS₄ × ℝ and find that there are only four isometries that survive the quotient with σ:

$$\chi_1 = u\partial_x + x\partial_u \tag{35}$$

$$= \ell \cos \theta \cosh \frac{2t}{\ell} \partial_t - \frac{1}{2} \ell^2 \sin \theta \sinh \frac{2t}{\ell} \partial_\theta \tag{36}$$

$$\chi_2 = v\partial_y + y\partial_v \tag{37}$$

$$= \ell \cosh \frac{2\phi}{\ell} \partial_\phi, \tag{38}$$

$$\chi_3 = u\partial_v - v\partial_u + x\partial_y - y\partial_x \tag{39}$$

$$= \ell \left(\sinh \frac{t}{\ell} \sinh \frac{\phi}{\ell} (\partial_\phi - \cosh \theta \partial_t) \right. \\ \left. + \cosh \frac{t}{\ell} \left(\cosh \frac{\phi}{\ell} (-\partial_t + \cos \theta \partial_\phi) + \ell \sin \theta \sinh \frac{\phi}{\ell} \partial_\theta \right) \right), \tag{40}$$

$$\chi_4 = u\partial_y + y\partial_u + x\partial_v + v\partial_x \tag{41}$$

$$= \ell \left(\sinh \frac{t}{\ell} \cosh \frac{\phi}{\ell} (\partial_\phi + \cosh \theta \partial_t) \right. \\ \left. + \cosh \frac{t}{\ell} \left(\sinh \frac{\phi}{\ell} (\partial_t + \cos \theta \partial_\phi) - \ell \sin \theta \cosh \frac{\phi}{\ell} \partial_\theta \right) \right). \tag{42}$$

Like in the case of NO-(AdS₃ × S²) on the boundary, these form $\mathfrak{sl}(2, \mathbb{R}) \oplus \mathbb{R}$ (though in the bulk). χ_4 vanishes at $\theta = 0$ and $t = -\phi$ or $\theta = \pi$ and $t = \phi$, reducing the isometries to just $\mathfrak{sl}(2, \mathbb{R})$.

It remains to verify that the boundaries of OB-dS₄ × ℝ qualify as asymptotically dS₄ despite the extra fifth dimension and its separation into two oppositely oriented Poincare patches. As already pointed out, it turns out that the fifth dimension coordinatized by φ is not supported on these boundaries because it is conformally suppressed. To see whether the conformal suppression is rapid enough not to affect the asymptotic symmetries, we can analytically continue the Brown-Henneaux boundary conditions from AdS₄ to de Sitter with global metric $ds^2 = \frac{\ell^2}{\cos^2 t} (-dt^2 + d\Omega_3^2)$. This reveals that since OB-dS₄ × ℝ's ℝ factor is independent of t, the only Brown-Henneaux condition that needs to be verified is $g_{AB} = (t \mp \pi/2)^{-2} \gamma_{AB} + \mathcal{O}(1)$, where γ_{AB} is the fixed metric on the spatial sphere at timelike infinity ($t \rightarrow \pm\pi/2$) and $x^A = (r, \Omega_2)$ [10]. This condition is clearly met by both OB-dS₄ × ℝ and regular dS₄ × ℝ. The same is true of dS₄ × S¹, which we will discuss later.

As for the effect of the opposite orientations caused by the σ quotient, since we know

this the quotient with σ reduces the bulk isometries to minimally $\mathfrak{sl}(2, \mathbb{R})$, it qualifies only as an asymptotically dS_4 with similarly reduced asymptotic symmetries. This is similar to the way that NO- AdS_3 is asymptotically AdS_3 despite only containing minimally an $\mathfrak{sl}(2, \mathbb{R})$ and its associated chiral Virasoro algebra.

In general, asymptotic symmetry spaces with reduced symmetries contain singularities that can be associated with the insertion of point particles with mass that have broken the removed isometries. As a result, these are usually excited states (e.g. BTZ compared to AdS_3). We shall soon see that perhaps a similar situation holds for $OB-dS_4 \times \mathbb{R}$, when it is identified as a false vacuum state at higher energy than the true vacuum state, where the singularities act as point particles.

B. The Bulk/Boundary Correspondence

Since σ is a subgroup of a double cover of AdS_3 's bulk isometry group, it can only produce fixed points on the boundary of NO- AdS_3 . This is similar to the case for self-dual AdS_3 , and as we found, both spaces have fixed points along two co-dimension one manifolds on their boundaries. Since we do not expect σ to also be a subgroup of $dS_4 \times \mathbb{R}$ or any of its covers, it should break the bulk spacetime into at least two manifolds.

We found in the previous section that the spacetime consists of two oppositely S^2 -oriented Poincaré patches with singularities at their horizons. The original original $dS_4 \times \mathbb{R}$ spacetime is severed along its Poincaré horizons (see Fig. 9) precisely because the σ is not a subgroup of $dS_4 \times \mathbb{R}$, and its quotient flips the orientation of the S^2 s of the two Poincaré patches of $OB-dS_4 \times \mathbb{R}$.

Note that, as shown in Fig. 9, antipodal static patches only experience one orientation of S^2 regardless of which pair of contracting and expanding Poincaré patches are chosen to cover $OB-dS_4 \times \mathbb{R}$. Heuristically, this is because the orientation they experience is uniquely determined by the singularity they asymptote to, and this singularity is contained in their Poincaré patch regardless of whether it is contracting or expanding.

Excising the Poincaré patch horizons allows us to now describe the structure of $OB-dS_4 \times \mathbb{R}$ in terms of two disjoint Poincaré patches. If boundary conditions are specified then the situation is similar to what occurs at the two fixed lines on the boundary of NO- $(AdS_3 \times S^2)$ to define two BCFT₂s: timelike geodesics that would normally cross this horizon in finite

proper time cannot do so now due to the boundary conditions.

Since NO-(AdS₃ × S²) and OB-dS₄ × ℝ are derived by foliating the same ℝ^{2,5} lightcone, they contain conformally flat patches that are also conformal to each other [40]. Specifically, these conformally flat patches correspond to the Rindler wedge of AdS₃ × S² and the static patch of dS₄ × ℝ [39].

The Rindler wedge of orientable or non-orientable AdS₃ × S² has metric,

$$ds^2 = - \left(\frac{r^2}{l^2} - 1 \right) dt^2 + \left(\frac{r^2}{l^2} \right)^{-1} dr^2 + r^2 d\phi^2 + l^2 d\Omega_2^2, \quad (43)$$

where $r \in (0, \ell)$, $t \in \mathbb{R}$, $\phi \in [0, 2\pi)$, and $d\Omega_2^2$ is the S² metric. The static patch metric of orientable dS₄ × ℝ or OB-dS₄ × ℝ is

$$ds^2 = - \left(1 - \frac{R^2}{L^2} \right) dt^2 + \left(1 - \frac{R^2}{L^2} \right)^{-1} dR^2 + R^2 d\Omega_2^2 + L^2 d\phi^2. \quad (44)$$

where $R \in (0, L)$, $t \in \mathbb{R}$, $\phi \in [0, 2\pi)$, and $d\Omega_2^2$ is the S² metric. Multiplying Eq. 44 with $\ell/r = R/L$ conformally maps it to Eq. 43 (see Appendix E for more details). These patches can be fully contained in the Poincaré patches of either the orientable and non-orientable AdS₃ × S², or dS₄ × ℝ and OB-dS₄ × ℝ. (In the OB-dS₄ × ℝ case, we coordinatize the antipodal static patch with domain $-L \geq R \geq 0$ instead of $0 \leq R \leq L$.)

Note that the conformal map is strictly between a Rindler patch of *the universal cover* of the AdS₃ × S² spacetime and a static patch of the dS₄ × ℝ spacetime, or in the non-orientable case, between a Rindler patch of *the orientable infinite cover* of NO-(AdS₃ × S²) obtained by unwrapping t and a static patch of OB-dS₄ × ℝ. This is because in dS₄ spacetime the future and past static patch horizons are independent and timelike separated. If the single cover of AdS₃ × S² or NO-(AdS₃ × S²) were considered, this property would be violated under the conformal map by their closed timelike curves.

Since the conformal map is between a single Rindler wedge and static patch, in general it is only useful for conformally defining a static patch vacuum. Extending the static patch vacuum to a global vacuum is not possible with two separate conformal maps if the former involves entanglement between states defined on antipodal static patches. However, for NO-(AdS₃ × S²) and OB-dS₄ × ℝ, this is not the case. Specifically, OB-dS₄ × ℝ actually consists of two distinct spacetimes separated by a lightlike singularity, which are not entangled with each other (i.e. any shared boundary conditions on the singularity must be Dirichlet boundary conditions). As a result, two separate conformal maps can map the

separable conformal vacuum state of NO- $(\text{AdS}_3 \times \text{S}^2)$ piecewise from each Rindler wedge to each antipodal static patch in OB- $\text{dS}_4 \times \mathbb{R}$.

This means that OB- $\text{dS}_4 \times \mathbb{R}$ supports the same conformal vacuum as the orientable infinite cover of NO- $(\text{AdS}_3 \times \text{S}^2)$. Namely, OB- $\text{dS}_4 \times \mathbb{R}$'s conformal vacuum bulk state is $|\omega\rangle |\bar{\omega}\rangle$, where $|\omega\rangle$ and $|\bar{\omega}\rangle$ are defined on antipodal static patches.

IV. DISCUSSION

We found that the Rindler boundary state of NO- AdS_3 with unwrapped t dimension has vanishing Hagedorn temperature due to supporting an infinitely long string. This must also be true for NO- $(\text{AdS}_3 \times \text{S}^2)$. Since the conformal map preserves this property, this means that the OB- $\text{dS}_4 \times \mathbb{R}$ conformal vacuum state is unstable to excitation. It is expected that this false vacuum state decays to a true vacuum that should have a bulk geometry with the same asymptotic boundaries.

$\text{dS}_4 \times \mathbb{R}$ has the same boundaries as OB- $\text{dS}_4 \times \mathbb{R}$, except that its past and future boundary are similarly oriented. As a result, it is a prospective true vacuum bulk geometry. If it is the correct state, then this suggests that under perturbation OB- $\text{dS}_4 \times \mathbb{R}$'s vanishing Hagedorn temperature is surpassed and the state undergoes decay through a phase transition to $\text{dS}_4 \times \mathbb{R}$, corresponding to “untwisting” its oppositely oriented boundaries. We leave determining the validity of such a decay pathway, and its mechanism, for future work.

It is important to note that the added \mathbb{R} dimension in OB- $\text{dS}_4 \times \mathbb{R}$ is crucial for connecting its vacuum with holography. While one could, in principle, construct a factorized vacuum on the space dS_4 with oppositely oriented boundaries it would be unclear how to infer anything about its holography. Furthermore, since NO- $(\text{AdS}_3 \times \text{S}^2)$ has a well-understood spectrum, the additional \mathbb{R} product space may allow for this conformal relationship to be used to determine the (excited-state) spectrum of OB- $\text{dS}_4 \times \mathbb{R}$ as well.

Finally, there is an interesting observation about the uniqueness of this dS_4 vacuum's construction from three dimensional AdS_3 . It is well known that AdS_3 is uniquely able to be described as a purely topological gauge theory [53, 54]. It is also only in three dimensions that the black hole of negatively curved spacetime, the BTZ spacetime, can be defined. Similarly, as we have pointed out throughout its derivation, it is only in three dimensions that a non-orientable AdS can be defined that is geometrically indistinguishable from regular

AdS, i.e. an orientifold of a double cover of AdS. In summary, it is these three spacetimes which are uniquely possible to define only in three dimensions that form the backbone of the conformal spectrum of the dS_4 vacuum.

—

This material is based upon work supported by the U.S. Department of Energy, Office of Science, Office of Advanced Scientific Computing Research, under the Quantum Testbed Pathfinder program. Support is also acknowledged from the U.S. Department of Energy, Office of Science, National Quantum Information Science Research Centers, Quantum System Accelerator (Award No. DE-SCL0000121). SAND2026-185120

Sandia National Laboratories is a multimission laboratory managed and operated by National Technology & Engineering Solutions of Sandia, LLC, a wholly owned subsidiary of Honeywell International Inc., for the U.S. Department of Energy’s National Nuclear Security Administration under contract DE-NA0003525. This paper describes objective technical results and analysis. Any subjective views or opinions that might be expressed in the paper do not necessarily represent the views of the U.S. Department of Energy or the United States Government.

Appendix A: NO-AdS₃

1. Iwasawa and Cartan coordinates

We will first look at the Cartan and Iwasawa coordinate of AdS₃. The Cartan coordinates are similar to the usual AdS₃ global coordinates, where any matrix in $SL(2, \mathbb{R})$ is represented as:

$$SL(2, \mathbb{R}) = \left\{ \begin{pmatrix} \cos \theta & -\sin \theta \\ \sin \theta & \cos \theta \end{pmatrix} \begin{pmatrix} \cosh \rho + \cos \alpha \sinh \rho & \sin \alpha \sinh \rho \\ \sin \alpha \sinh \rho & \cosh \rho - \cos \alpha \sinh \rho \end{pmatrix} : \right. \quad (A1)$$

$$\left. \rho \geq 0, \alpha \in [0, 2\pi), \theta \in [0, 2\pi). \right\} \quad (A2)$$

The metric in these coordinates is

$$ds^2 = -\cosh^2 \rho d\theta^2 + d\rho^2 + \sinh^2 \rho d(\theta - \alpha)^2. \quad (A3)$$

This allows us to identify $\tau = \theta, \phi = \theta - \alpha$ is the usual AdS₃ global coordinates. The boundary of the spacetime is located only as $\rho \rightarrow +\infty$, and so the completion of the

spacetime is simply:

$$\overline{\text{SL}(2, \mathbb{R})} = \left\{ \begin{pmatrix} \cos \theta & -\sin \theta \\ \sin \theta & \cos \theta \end{pmatrix} \begin{pmatrix} \cosh \rho + \cos \alpha \sinh \rho & \sin \alpha \sinh \rho \\ \sin \alpha \sinh \rho & \cosh \rho - \cos \alpha \sinh \rho \end{pmatrix} : \right. \quad (\text{A4})$$

$$\left. \rho \in [0, +\infty], \alpha \in [0, 2\pi), \theta \in [0, 2\pi). \right\} \quad (\text{A5})$$

The boundary topology is $\mathbb{S}^1 \times \mathbb{S}^1$ parameterized by α, θ at $\rho = +\infty$.

The Iwasawa coordinates are also global, and take the form

$$\text{SL}(2, \mathbb{R}) = \left\{ \begin{pmatrix} \frac{\cos \theta + x \sin \theta}{r} & \frac{-\sin \theta + x \cos \theta}{r} \\ r \sin \theta & r \cos \theta \end{pmatrix} : \theta \in [0, 2\pi), x \in \mathbb{R}, r > 0 \right\}. \quad (\text{A6})$$

The metric in these coordinates is from the determinant of the differential in Iwasawa coordinates

$$\left(\frac{(-\sin \theta + x \cos \theta)d\theta + dx \sin \theta}{r} - \frac{dr}{r^2}(\cos \theta + x \sin \theta) \right) (-r \sin \theta d\theta + dr \cos \theta) - \quad (\text{A7})$$

$$\left(\frac{(-\cos \theta - x \sin \theta)d\theta + dx \cos \theta}{r} - \frac{dr}{r^2}(-\sin \theta + x \cos \theta) \right) (r \cos \theta d\theta + dr \sin \theta) \quad (\text{A8})$$

We can compute terms individually:

$$d\theta^2 : (-\sin \theta + x \cos \theta)(-\sin \theta) - (-\cos \theta - x \sin \theta) \cos \theta = 1 \quad (\text{A9})$$

$$dr^2 : \frac{1}{r^2} (-(\cos \theta + x \sin \theta) \cos \theta + (-\sin \theta + x \cos \theta) \sin \theta) = -\frac{1}{r^2} \quad (\text{A10})$$

$$dx^2 : 0 \quad (\text{A11})$$

$$dx d\theta : -\sin^2 \theta - \cos^2 \theta = -1 \quad (\text{A12})$$

$$dx dr : \frac{1}{r} (\sin \theta \cos \theta - \cos \theta \sin \theta) = 0 \quad (\text{A13})$$

$$dr d\theta : \frac{1}{r} ((-\sin \theta + x \cos \theta) \cos \theta + \sin \theta (\cos \theta + x \sin \theta)) + \quad (\text{A14})$$

$$\frac{1}{r} ((\cos \theta + x \sin \theta) \sin \theta + \cos \theta (-\sin \theta + x \cos \theta)) = \frac{2x}{r}. \quad (\text{A15})$$

The full metric is then:

$$\text{SL}(2, \mathbb{R}) \rightarrow ds^2 = -d\theta^2 + dx d\theta - \frac{2x}{r} d\theta dr + \frac{dr^2}{r^2} \quad (\text{A16})$$

$$r > 0, \theta \in [0, 2\pi), x \in \mathbb{R}. \quad (\text{A17})$$

The boundary is a little trickier as we have boundaries in the half-plane defined by (r, x) . The only non-trivial limits would be $x/r = \text{const}$, which are lines which limit in one direction

to $r = x = 0$ and in the other direction to a line of infinities. This is the standard completion of the Poincare half-plane, and the line plus point which are inserted are equivalent to the circular boundary in the Poincare disk compactification of a plane utilized in ordinary AdS₃ global coordinates. The completion of $\text{SL}(2, \mathbb{R})$ is then:

$$\overline{\text{SL}(2, \mathbb{R})} \cong \left\{ \begin{pmatrix} \frac{\cos \theta}{r} + \chi \sin \theta & -\frac{\sin \theta}{r} + \chi \cos \theta \\ r \sin \theta & r \cos \theta \end{pmatrix} : \theta \in [0, 2\pi), \right. \quad (\text{A18})$$

$$\left. (r, \chi) \in (\mathbb{R}^+ \times \mathbb{R}) \cup (\{\infty\} \times \mathbb{R}) \cup \{(0, 0)\} \cong \overline{\mathbb{D}^2} \right\}. \quad (\text{A19})$$

Note that the compactification is carried out entirely in the (r, χ) plane, independent of the value of θ . Proceeding as before, we can write the metric for $\overline{\text{SL}(2, \mathbb{R})}$ as:

$$\overline{\text{SL}(2, \mathbb{R})} \rightarrow ds^2 = \frac{dr^2}{r^2} - d\theta^2 - \chi d\theta dr + r d\chi d\theta \quad (\text{A20})$$

$$\theta \in [0, 2\pi), (r, \chi) \in (\mathbb{R}^+ \times \mathbb{R}) \cup (\{\infty\} \times \mathbb{R}) \cup \{(0, 0)\}. \quad (\text{A21})$$

This also has the same boundary topology, $\mathbb{S}^1 \times \mathbb{S}^1$ as expected.

2. Mobius construction

Since the Iwasawa and Cartan constructions are equivalent, we can in principle construct NO-AdS₃ from either coordinate system. The construction is only naturally manifest in the Iwasawa form, however.

To see why, let us look at the Cartan case first. Here, we have a natural cylinder spanned by (θ, ρ) . The typical Mobius identification would then be:

$$(\theta, \rho) \xrightarrow{\text{glue}} (\theta + 2\pi, \rho^{-1}). \quad (\text{A22})$$

The inverse is present here since $\rho \geq 0$, and the usual $x \sim -x$ fiber identification for a Mobius strip can be seen as $\rho \equiv e^\xi$ wherein $\xi \sim -\xi$ is the same as $\rho \sim \rho^{-1}$. The issue here is that $\rho = 0$, a point in the bulk, is glued to $\rho = +\infty$, a point in the conformal boundary, which would break the geometry of the spacetime.

Consider now the Iwasawa case. There are now two possible "fiber" directions, r, χ and one angular direction θ . If we were to take r

$$(\theta, r) \xrightarrow{\text{glue}} (\theta + 2\pi, r^{-1}), \quad (\text{A23})$$

we now have $r = 0, \infty$ both as boundary point, however they are not the same "kind" of boundary since $r = 0$ limits to a single point where $r = \infty$ limits to a line in χ . Discarding this option, the only remaining option would be the gluing:

$$(\theta, \chi) \xrightarrow{\text{glue}} (\theta + 2\pi, -\chi). \quad (\text{A24})$$

This is finally a valid gluing topologically.

We note, however, that the line element is not invariant under this change, and so there is no global line element on this space. Instead, we can define two patches with the following domains, metrics, and overlaps, to get the full non-orientable construction:

Patch 1

$$ds^2 = \frac{dr^2}{r^2} - d\theta^2 - (\chi d\theta dr - r d\chi d\theta), \quad r > 0, \quad \chi \in \mathbb{R}, \theta \in (0, 2\pi) \quad (\text{A25})$$

Patch 2

$$ds^2 = \frac{dr'^2}{r'^2} - d\theta'^2 - (\chi' d\theta' dr' - r' d\chi' d\theta'), \quad r' < 0, \quad \chi' \in \mathbb{R}, \theta' \in (-\pi, \pi) \quad (\text{A26})$$

Overlap

$$(r', \theta', \chi') = (-r, \theta - \pi, -\chi). \quad (\text{A27})$$

The expressions in Eqs A25-A27 define the bulk geometry of NO-AdS₃: it is non-orientable, smooth, and locally AdS₃. The global topology is

$$\text{NO} - \text{AdS}_3 \cong \mathcal{M} \times \mathbb{R}^+. \quad (\text{A28})$$

3. Torus boundary

To find the boundary topology, we note that the boundary has two parts: $r = +\infty$ and $r = 0$. The prior is a line with $\chi \in \mathbb{R}$ and follows the ordinary Mobius twist rules. The fundamental polygon here has opposite arrows for the χ twist at $\theta = 0, 2\pi$ and no identification at $\chi \rightarrow \pm\infty$. The remaining point on the boundary $r = 0, \chi = 0$ serves to glue the two ends of the Mobius strip at $r = \infty$ such that $r = 0, \chi = 0$ serves really as $\chi = \infty$. This allows to add aligned arrows on the fundamental polygon at $\chi = \pm\infty$ and hence the resulting boundary topology is that of an orientable double cover of a Klein bottle, which is a torus:

$$\partial(\text{NO} - \text{AdS}_3) \cong S^1 \times S^1. \quad (\text{A29})$$

Appendix B: NO-(AdS₃ × S²) as two glued patches

As in Section III A we begin with two sections of the $\mathbb{R}^{2,5}$ lightcone related to each other by the simultaneous exchange $(u, v) \leftrightarrow (-x, -y)$ and Wick rotation $r \leftrightarrow ir$. Building on the Poincare patch construction in [41] for NO-AdS₃, we construct a double cover of AdS₃ × S² by transforming the two sections of the lightcone via a piecewise map $\Phi = \{\Phi_+, \Phi_-\}$ defined below.

Following the notation in [41], let $(a, b, c, d) := (u + x, v + y, v - y, x - u)$ denote the lightcone coordinates on the $\mathbb{R}^{2,2}$ factor. Additionally, let \mathbb{R}^3 and its Wick rotation be covered by spherical coordinates (r, θ, ϕ) . On the $\mathbb{R}^{2,2}$ factor, Φ acts as in Section II A:

$$\Phi_{\pm} : (a, b, c, d) \longrightarrow (\pm a^2, \pm ab, \pm ab + c, \pm b^2 + d) =: (A, B, C, D) \quad (\text{B1})$$

On the \mathbb{R}^3 factor (and its Wick-rotated counterpart), the action of Φ is defined (in spherical coordinates) as follows:

$$\Phi_+ : \begin{cases} (r, \theta, \phi) \longrightarrow (r, \theta, \phi) \\ (ir, \theta, \phi) \longrightarrow (r, \theta, \phi) \end{cases} \quad (\text{B2})$$

$$\Phi_- : \begin{cases} (r, \theta, \phi) \longrightarrow (ir, \theta, \phi) \\ (ir, \theta, \phi) \longrightarrow (ir, \theta, \phi) \end{cases} \quad (\text{B3})$$

We introduce the following metric on the resulting space:

$$ds_{\pm}^2 = d(\pm a^2)d(\pm b^2 + d) - d(\pm ab)d(\pm ab + c)d\tilde{r}^2 + \tilde{r}^2 d\Omega^2 \quad (\text{B4})$$

$$= dAdD - dBdC + d\tilde{r}^2 + \tilde{r}^2 d\Omega_2^2 \quad (\text{B5})$$

where we use the complex coordinate \tilde{r} to denote the real and imaginary image of the radial coordinate under Φ_{\pm} . Taken together, the image of Φ_{\pm} covers the entire $\mathbb{R}^{2,5}$ lightcone twice. Upon restring to the appropriate subregions, the image of the map Φ_+ covers the $A > 0$ regions of each hyperbola $AD - BC = \pm\epsilon$ twice. Likewise, the image of Φ_- covers the $A < 0$ regions of each hyperbola twice. The relevant AdS₃ × S² restrictions are

$$AD - BC = \pm a(ab - dc) = \mp\epsilon \quad (\text{B6})$$

$$\tilde{r}^2 = \pm\epsilon \quad (\text{B7})$$

from which we obtain two AdS₃ hyperboloids, and two copies of S² related by Wick rotation of the \tilde{r} coordinate. In the Poincaré coordinates introduced in Section II A 4-5, the metric takes the form

$$ds^2 = \begin{cases} \frac{1}{y^2} (-d\tau^2 + dx^2 + \epsilon dy^2) + \tilde{r}^2 d\Omega_2^2 & \text{for } y > 0, \tilde{r} > 0, AD - BC = -\epsilon, \tilde{r}^2 = \epsilon \\ \frac{1}{y^2} (d\tau^2 - dx^2 - \epsilon dy^2) - \tilde{r}^2 d\Omega_2^2, & \text{for } y > 0, -i\tilde{r} > 0, AD - BC = \epsilon, \tilde{r}^2 = -\epsilon \end{cases} \quad (\text{B8})$$

As described in Section II A, to obtain an AdS₃ factor with the original signature, we allow the Poincaré patch of the Φ_- branch to be covered by $y < 0$, giving:

$$ds^2 = \begin{cases} \frac{1}{y^2} (-d\tau^2 + dx^2 + \epsilon dy^2) + \tilde{r}^2 d\Omega_2^2, & \text{for } y > 0, \tilde{r} > 0, AD - BC = -\epsilon, \tilde{r}^2 = \epsilon \\ \frac{1}{y^2} (-dx^2 + d\tau^2 + \epsilon dy^2) - \tilde{r}^2 d\Omega_2^2, & \text{for } y < 0, -i\tilde{r} > 0, AD - BC = -\epsilon, \tilde{r}^2 = -\epsilon \end{cases} \quad (\text{B9})$$

It remains to fix the signature of the S² metric. To do this, on the $y < 0$ patch we introduce a simultaneous Wick rotation $\tilde{r}' = i\tilde{r}$. The metric becomes

$$ds^2 = \begin{cases} \frac{1}{y^2} (-d\tau^2 + dx^2 + \epsilon dy^2) + \tilde{r}'^2 d\Omega_2^2, & \text{for } y > 0, \tilde{r}' > 0, AD - BC = -\epsilon, \tilde{r}'^2 = \epsilon \\ \frac{1}{y^2} (-dx^2 + d\tau^2 + \epsilon dy^2) + \tilde{r}'^2 d\Omega_2^2, & \text{for } y < 0, \tilde{r}' < 0, AD - BC = -\epsilon, \tilde{r}'^2 = \epsilon \end{cases} \quad (\text{B10})$$

Note that $\tilde{r}' < 0$ since $\tilde{r}' = i\tilde{r} = i(ir) = -r$, and $r > 0$. The resulting metric is the space NO-(AdS₃ × S²) described in Section II E.

Appendix C: dS₄ × ℝ Bulk Isometry Group and σ

σ is not a subgroup of the bulk isometry group of dS₄ × ℝ or any of its higher covers. This can be verified by noting that it cannot be expressed in global coordinates of dS₄ × ℝ:

$$u = \ell \sinh(t/\ell), \quad x = \ell \cosh(t/\ell) \cos(\theta), \quad (\text{C1})$$

$$v = \ell \cosh(\phi/\ell), \quad y = \ell \sinh(\phi/\ell), \quad (\text{C2})$$

$$a = \ell \cosh(t/\ell) \sin(\theta) \cos(\alpha), \quad b = \ell \cosh(t/\ell) \sin(\theta) \sin(\alpha) \cos(\beta), \quad (\text{C3})$$

$$c = \ell \cosh(t/\ell) \sin(\theta) \sin(\alpha) \sin(\beta) \quad (\text{C4})$$

To attempt to express σ in these coordinates one must choose $\sinh(t/\ell) \leftrightarrow -\cosh(it/\ell) \cos(\theta)$ to get $u \leftrightarrow -x$ and $\ell \rightarrow i\ell$ to get $(a, b, c) \rightarrow i(a, b, c)$ (it is not possible to use α and β to affect this Wick rotation). However, it is easy to find that these two contradict each other and are incompatible.

Appendix D: OB-dS₄ × ℝ Poincaré Patch Derivation

Consider

$$\underbrace{-u^2 + x^2 + a^2 + b^2 + c^2}_{=+\epsilon} \underbrace{-v^2 + y^2}_{=-\epsilon} = 0, \quad (\text{D1})$$

and

$$\underbrace{-u^2 + x^2 + a^2 + b^2 + c^2}_{=-\epsilon} \underbrace{-v^2 + y^2}_{=+\epsilon} = 0. \quad (\text{D2})$$

We therefore consider the same double cover of the $\mathbb{R}^{2,5}$ lightcone (and its Wick rotation) as described in Appendix B, but with restrictions to the dS₄ × ℝ subspace, rather than the AdS₃ × S² subspace. In particular, we consider the restrictions

$$AD = \pm \tilde{r}^2 - (\pm)\epsilon \quad (\text{D3})$$

$$BC = \pm\epsilon \quad (\text{D4})$$

We again consider a disjoint subset of the lightcone obtained via changing the sign of ϵ in the embedding constraints. The new subset is similarly related to the first by performing $\sigma(u, v, x, y) = -(x, y, u, v)$ along with a Wick rotation of the (a, b, c) coordinates: The simultaneous change in sign of ϵ and \tilde{r}^2 results in two oppositely oriented copies of dS₄. We introduce Poincaré coordinates on the two dS₄ copies as follows:

$$A = \pm 1/\eta, \quad B = \pm L \exp -\phi, \quad (\text{D5})$$

$$C = L \exp \phi, \quad D = \frac{X^2 - \epsilon \eta^2}{\eta} \quad (\text{D6})$$

$$\tilde{r} = X/\eta \quad (\text{D7})$$

$$ds^2 = \begin{cases} \frac{1}{\eta^2} (-d\eta^2 + dX^2 + X^2 d\Omega_2^2 + \eta^2 L^2 d\phi^2) & \text{for } \eta > 0, X > 0, AD = X^2 - \epsilon \\ -\frac{1}{\eta^2} (-d\eta^2 + dX^2 + X^2 d\Omega_2^2 + \eta^2 L^2 d\phi^2) & \text{for } \eta > 0, -iX > 0, AD = -X^2 + \epsilon \end{cases} \quad (\text{D8})$$

We begin returning these to consistent signatures by first setting the $\eta < 0$ on the second branch, and Wick rotating L :

$$A = 1/\eta, \quad B = \frac{+1}{-i}L \exp -\phi \quad (\text{D9})$$

$$C = \frac{+1}{+i}L \exp \phi, \quad D = \frac{\pm X^2 - \epsilon \eta^2}{\eta} \quad (\text{D10})$$

$$\tilde{r} = \pm X/\eta \quad (\text{D11})$$

where $\epsilon = L^2$, so that $L \rightarrow iL$ implies $\epsilon \rightarrow -\epsilon$. The induced metrics are

$$ds^2 = \begin{cases} \frac{1}{\eta^2} (-d\eta^2 + dX^2 + X^2 d\Omega_2^2 + \eta^2 L^2 d\phi^2), & \eta > 0, X > 0, AD = X^2 - \epsilon \\ \frac{1}{\eta^2} (-d\eta^2 - dX^2 - X^2 d\Omega_2^2 + \eta^2 L^2 d\phi^2), & \eta < 0, -iX > 0, AD = -X^2 - \epsilon, \end{cases} \quad (\text{D12})$$

Note that the Wick rotation of L in the minus branch similarly occurs in the construction of NO-(AdS₃ × S²), where in that case it corresponds to a Wick rotation of the S² factor, rather than the \mathbb{R} factor, but similarly ensures that $\epsilon \rightarrow -\epsilon$. To obtain an dS₄ metric on both sides we need to perform another Wick rotation of X on the second patch of the covering map. The result is that $dX^2 + X^2 d\Omega^2 \rightarrow -dX^2 - X^2 d\Omega^2$. In addition, since on the second patch we have $X = ir$, we find that $X \rightarrow i(ir) = -r < 0$.

As a result,

$$ds^2 = \begin{cases} \frac{1}{\eta^2} (-d\eta^2 + dX^2 + X^2 d\Omega_2^2 + \eta^2 L^2 d\phi^2), & \eta > 0, X > 0, AD = X^2 - \epsilon, \\ \frac{1}{\eta^2} (-d\eta^2 + dX^2 + X^2 d\Omega_2^2 + \eta^2 L^2 d\phi^2), & \eta < 0, X < 0, AD = X^2 - \epsilon. \end{cases} \quad (\text{D13})$$

Note that instead choosing the other Poincaré patch with the same spacelike boundary corresponds to exchanging $u + x \leftrightarrow u - x$. This is equivalent to $A \leftrightarrow D$ above, which does not effect the derivation. As a result, Poincaré patches with the same spacelike boundary share the same orientation (denoted by $X > 0$ or $X < 0$ in Fig. 9).

Appendix E: Rindler-AdS₃ × S² ≅ Static-dS₄ × \mathbb{H}^1

As demonstrated in [40], any two spacetimes which are conformally flat can be embedded in an $\mathbb{R}^{(2,D-2)}$ lightcone. Moreover, any two spacetimes which can be embedded in the same lightcone can be related to one another via a Weyl transformation. This can be used to establish conformal equivalences between many conformally flat spaces. Additionally, since

local geometry is preserved under quotients, this method can also be used to establish the conformal equivalence of quotients of the embedded spaces. We first use this embedding space formalism to demonstrate the known conformal relationship between Rindler wedges of $\text{AdS}_3 \times \text{S}^2$ and the static patches of $\text{dS}_4 \times \text{S}^1$. We then establish a conformal relationship between quotients of their double covers, namely those which produce $\text{NO-AdS}_3 \times \text{S}^2$ and $\text{OB-dS}_4 \times \mathbb{H}^1$.

We consider a lightcone through the origin of $\mathbb{R}^{2,5}$ given by

$$-u^2 - v^2 + x^2 + y^2 + a^2 + b^2 + c^2 = 0 \quad (\text{E1})$$

$\text{AdS}_3 \times \text{S}^2$ is obtained by the additional constraints

$$\underbrace{-u^2 + x^2 - v^2 + y^2}_{=-l^2} + \underbrace{a^2 + b^2 + c^2}_{=l^2} = 0. \quad (\text{E2})$$

We introduce an additional constraint to parameterize the AdS Rindler wedges:

$$\underbrace{-u^2 + x^2}_{=r^2-l^2} + \underbrace{-v^2 + y^2}_{=-r^2} + \underbrace{a^2 + b^2 + c^2}_{=l^2} = 0, \quad (\text{E3})$$

where r is the Rindler radial coordinate. The induced metric ds^2 on this section of the lightcone is

$$ds^2 = - \left(\frac{r^2}{l^2} - 1 \right) dt^2 + \left(\frac{r^2}{l^2} - 1 \right)^{-1} dr^2 + r^2 d\phi^2 + l^2 d\Omega_2^2. \quad (\text{E4})$$

Similarly, $\text{dS}_4 \times \mathbb{R}$ is embedded into the lightcone with a set of constraints:

$$\underbrace{-u^2 + x^2 + a^2 + b^2 + c^2}_{=L^2} - \underbrace{v^2 + y^2}_{=-L^2} = 0 \quad (\text{E5})$$

To parameterize the static patches, we introduce the additional constraint

$$\underbrace{-u^2 + x^2}_{=-R^2+L^2} + \underbrace{a^2 + b^2 + c^2}_{=R^2} - \underbrace{v^2 + y^2}_{=-L^2} = 0 \quad (\text{E6})$$

where R is the static patch radial coordinate. The induced metric $d\tilde{s}^2$ is

$$d\tilde{s}^2 = - \left(1 - \frac{R^2}{L^2} \right) dt^2 + \left(1 - \frac{R^2}{L^2} \right)^{-1} dR^2 + R^2 d\Omega_2^2 + L^2 d\phi^2. \quad (\text{E7})$$

It is clear from (E3) and (E6) that the set of constraints are identical, with the roles of the radial coordinates and curvature radii interchanged, i.e. $(r, l) \leftrightarrow (L, R)$. Indeed, we also see that metrics (E4) and (E7) are related by a Weyl rescaling $\Omega^2 = \left(\frac{l}{r}\right)^2 = \left(\frac{R}{L}\right)^2$. In particular,

$$d\tilde{s}^2 = \left(\frac{l}{r}\right)^2 \cdot ds^2 \Big|_{\substack{r=L \\ l=R}} \quad (\text{E8})$$

Finally, since the induced metrics on the Rindler wedges and static patches of $\text{AdS}_3 \times \text{S}^2$ and $\text{dS}_4 \times \mathbb{R}$ (resp.) are locally identical to those on their non-orientable counterparts, NO- $(\text{AdS}_3 \times \text{S}^2)$ and OB- $\text{dS}_4 \times \mathbb{R}$, the same conformal relationship holds for them as well.

-
- [1] NA Chernikov and EA Tagirov. Quantum theory of scalar field in de Sitter space-time. In *Annales de l'institut Henri Poincaré. Section A, Physique Théorique*, volume 9, pages 109–141, 1968.
- [2] Christiane Schomblond and Philippe Spindel. Conditions d'unicité pour le propagateur $\delta^1(x, y)$ du champ scalaire dans l'univers de de Sitter. In *Annales de l'institut Henri Poincaré. Section A, Physique Théorique*, volume 25, pages 67–78, 1976.
- [3] Timothy S Bunch and Paul CW Davies. Quantum field theory in de Sitter space: renormalization by point-splitting. *Proceedings of the Royal Society of London. A. Mathematical and Physical Sciences*, 360(1700):117–134, 1978.
- [4] Gary W Gibbons and Stephen W Hawking. Cosmological event horizons, thermodynamics, and particle creation. *Physical Review D*, 15(10):2738, 1977.
- [5] Emil Mottola. Particle creation in de Sitter space. *Physical Review D*, 31(4):754, 1985.
- [6] Bruce Allen. Vacuum states in de Sitter space. *Physical Review D*, 32(12):3136, 1985.
- [7] Tom Banks, Willy Fischler, and Sonia Paban. Recurrent nightmares?: Measurement theory in de Sitter space. *Journal of High Energy Physics*, 2002(12):062, 2003.
- [8] Raphael Bousso. Bekenstein bounds in de Sitter and flat space. *Journal of High Energy Physics*, 2001(04):035, 2001.
- [9] Raphael Bousso. Adventures in de Sitter space. *arXiv preprint hep-th/0205177*, 2002.
- [10] Andrew Strominger. The ds/cft correspondence. *Journal of High Energy Physics*, 2001(10):034, 2001.
- [11] Marcus Spradlin, Andrew Strominger, and Anastasia Volovich. De Sitter space. In *Unity from Duality: Gravity, Gauge Theory and Strings: Les Houches Session LXXVI, 30 July–31 August 2001*, pages 423–453. Springer, 2003.

- [12] Tom Banks. Cosmological breaking of supersymmetry? *International Journal of Modern Physics A*, 16(05):910–921, 2001.
- [13] Edward Witten. Quantum gravity in de Sitter space. *arXiv preprint hep-th/0106109*, 2001.
- [14] Tom Banks and Willy Fischler. M-theory observables for cosmological space-times. *arXiv preprint hep-th/0102077*, 2001.
- [15] Raphael Bousso. The holographic principle. *Reviews of modern physics*, 74(3):825, 2002.
- [16] Tom Banks and W Fischler. The holographic spacetime model of cosmology. *International Journal of Modern Physics D*, 27(14):1846005, 2018.
- [17] Cesar Arias, Felipe Diaz, and Per Sundell. De Sitter space and entanglement. *Classical and Quantum Gravity*, 37(1):015009, 2019.
- [18] Tom Banks and Willy Fischler. Holographic space-time, Newtons Law, and the dynamics of horizons. *arXiv preprint arXiv:2003.03637*, 2020.
- [19] Gabriel Arenas-Henriquez, Felipe Diaz, and Per Sundell. Logarithmic corrections, entanglement entropy, and UV cutoffs in de Sitter spacetime. *Journal of High Energy Physics*, 2022(8):1–28, 2022.
- [20] LH Ford. Quantum instability of de Sitter spacetime. *Physical Review D*, 31(4):710, 1985.
- [21] Ignatios Antoniadis, J Iliopoulos, and TN Tomaras. Quantum instability of de Sitter space. *Physical review letters*, 56(13):1319, 1986.
- [22] Emmanuel G Floratos, J Iliopoulos, and Th N Tomaras. Tree-level scattering amplitudes in de Sitter space diverge. *Physics Letters B*, 197(3):373–378, 1987.
- [23] Arvind Rajaraman. De Sitter space is unstable in quantum gravity. *Physical Review D*, 94(12):125025, 2016.
- [24] Mir Faizal, Sudhaker Upadhyay, and Bhabani Prasad Mandal. IR finite graviton propagators in de Sitter spacetime. *The European Physical Journal C*, 76(4):189, 2016.
- [25] Juan Maldacena and Carlos Nunez. Supergravity description of field theories on curved manifolds and a no go theorem. *International Journal of Modern Physics A*, 16(05):822–855, 2001.
- [26] Laura Covi, Marta Gomez-Reino, Christian Gross, Jan Louis, Gonzalo A Palma, and Claudio A Scrucca. de Sitter vacua in no-scale supergravities and Calabi-Yau string models. *Journal of High Energy Physics*, 2008(06):057–057, 2008.
- [27] Xingang Chen, Gary Shiu, Yoske Sumitomo, and S-H Henry Tye. A global view on the search for de Sitter vacua in (type IIA) string theory. *Journal of High Energy Physics*, 2012(4):1–20,

- 2012.
- [28] Iosif Bena, Mariana Grana, Stanislav Kuperstein, and Stefano Massai. Giant tachyons in the landscape. *Journal of High Energy Physics*, 2015(2):1–26, 2015.
 - [29] Georges Obied, Hiroshi Ooguri, Lev Spodyneiko, and Cumrun Vafa. De Sitter space and the swampland. *arXiv preprint arXiv:1806.08362*, 2018.
 - [30] T Banks and Willy Fischler. An holographic cosmology. *arXiv preprint hep-th/0111142*, 2001.
 - [31] Maulik Parikh and Erik Verlinde. De Sitter holography with a finite number of states. *Journal of High Energy Physics*, 2005(01):054, 2005.
 - [32] T Banks and W Fischler. Holographic cosmology 3.0. *Physica scripta*, 2005(T117):56, 2005.
 - [33] Tom Banks and Willy Fischler. Holographic inflation revised. *The philosophy of cosmology*, pages 241–262, 2017.
 - [34] Leonard Susskind. De Sitter space, double-scaled SYK, and the separation of scales in the semiclassical limit. *arXiv preprint arXiv:2209.09999*, 2022.
 - [35] Leonard Susskind. Black holes hint towards de Sitter matrix theory. *Universe*, 9(8):368, 2023.
 - [36] Leonard Susskind. Entanglement and chaos in de Sitter holography: An SYK example. *arXiv preprint arXiv:2109.14104*, 2021.
 - [37] Edgar Shaghoulian. The central dogma and cosmological horizons. *Journal of High Energy Physics*, 2022(1):1–31, 2022.
 - [38] Edgar Shaghoulian and Leonard Susskind. Entanglement in de Sitter space. *Journal of High Energy Physics*, 2022(8):1–23, 2022.
 - [39] Dionysios Anninos, Sean A Hartnoll, and Diego M Hofman. Static patch solipsism: conformal symmetry of the de Sitter worldline. *Classical and Quantum Gravity*, 29(7):075002, 2012.
 - [40] Sam Leuven, Erik Verlinde, and Manus Visser. Towards non-AdS holography via the long string phenomenon. *JHEP*, 06:097, 2018.
 - [41] Shivesh Pathak and Lucas Kocia Kovalsky. Non-orientable AdS₃ and its holography. *arXiv preprint arXiv:2404.12546*, 2024.
 - [42] Vijay Balasubramanian, Jamie Parsons, and Simon F Ross. States of a chiral 2d CFT. *Classical and Quantum Gravity*, 28(4):045004, 2011.
 - [43] O Coussaert and M Henneaux. Self-dual solutions of 2+ 1 Einstein gravity with a negative cosmological constant. *arXiv preprint hep-th/9407181*, 1994.
 - [44] Si Chen, Donald M Witt, and Steven S Plotkin. Quantizing models of (2+ 1)-dimensional

- gravity on non-orientable manifolds. *Classical and Quantum Gravity*, 31(5):055008, 2014.
- [45] John L Cardy. Boundary conditions in conformal field theory. In *Integrable systems in quantum field theory and statistical mechanics*, pages 127–148. Elsevier, 1989.
- [46] Vijay Balasubramanian, Jan de Boer, MM Sheikh-Jabbari, and Joan Simón. What is a chiral 2d CFT? and what does it have to do with extremal black holes? *Journal of High Energy Physics*, 2010(2):1–20, 2010.
- [47] Wei Li, Wei Song, and Andrew Strominger. Chiral gravity in three dimensions. *Journal of High Energy Physics*, 2008(04):082, 2008.
- [48] Andrew Strominger. A simple proof of the chiral gravity conjecture. *arXiv preprint arXiv:0808.0506*, 2008.
- [49] John Cardy. Boundary conformal field theory. *arXiv preprint hep-th/0411189*, 2004.
- [50] Tadashi Takayanagi. Holographic dual of a boundary conformal field theory. *Physical review letters*, 107(10):101602, 2011.
- [51] Ralph Blumenhagen, Dieter Lüst, and Stefan Theisen. *Basic concepts of string theory*. Springer Science & Business Media, 2012.
- [52] J David Brown and Marc Henneaux. Central charges in the canonical realization of asymptotic symmetries: An example from three dimensional gravity. *Communications in Mathematical Physics*, 104:207–226, 1986.
- [53] Edward Witten. 2+ 1 dimensional gravity as an exactly soluble system. *Nuclear Physics B*, 311(1):46–78, 1988.
- [54] Edward Witten. Three-dimensional gravity revisited. *arXiv preprint arXiv:0706.3359*, 2007.